Trabajo Fin de Grado
Grado en Ingeniería Química

Review of models and procedures for the measurement of reflectance in CSP plants

Autor: Alejandro Álvaro Llorente Carrión

Tutores: Manuel Silva Pérez, Dr. Aránzazu Fernández García

Departamento de Ingeniería Energética
Escuela Técnica Superior de Ingeniería
Universidad de Sevilla

Sevilla, 2020

Trabajo Fin de Grado

Grado en Ingeniería Química

Revisión de modelos y procedimientos para la medida de la reflectancia en plantas CSP

Autor:

Alejandro Álvaro Llorente Carrión

Tutor:

Manuel Silva Pérez

Profesor titular

Dr. Aránzazu Fernández García

CIEMAT – Plataforma Solar de Almería

Dpto. de Ingeniería Energética

Escuela Técnica Superior de Ingeniería

Universidad de Sevilla

Sevilla, 2020

Trabajo Fin de Grado: Review of models and procedures for the measurement of reflectance in CSP plants

Autor: Alejandro Álvaro Llorente Carrión

Tutores: Manuel Silva Pérez

Dr. Aránzazu Fernández García

El tribunal nombrado para juzgar el Trabajo Fin de Grado arriba indicado, compuesto por los siguientes miembros:

Presidente:

Vocales:

Secretario:

Acuerdan otorgarle la calificación de:

Sevilla, 2020

El Secretario del Tribunal

A mi Familia

A mi Gente

A mis compañeros de este tan largo y divertido viaje

A ti

Agradecimientos

En primer lugar, quisiera agradecer a los tutores de este trabajo de fin de grado, D. Manuel Silva Pérez y Dña. Arantxa Fernández García su tiempo, predisposición y confianza depositada en mi persona desde el primer momento. Sin apenas conocerme de nada, me han dado total libertad para la confección de este trabajo. Por circunstancias personales, el desarrollo de este se tuvo que dejar a mitad de camino, y se retomó dos años después con todo el apoyo de ambos tutores. Personalmente, situaciones como esta dejan entrever la calidad profesional y humana de las personas. Mis más sinceras gracias.

Ha sido un largo camino, desde el año 2003, en el que empiezo la licenciatura en Ingeniería Química, hasta el año 2020 en el que se culmina el camino, muchas personas, parejas, experiencias, trabajos, prácticas, profesores y proyectos han pasado por delante de mí. Tantos compañeros de estudio he visto pasar, siempre me quedo con lo mejor de haber estudiado con personas de mi generación y de 10 años atrás, una experiencia muy divertida y enriquecedora. No es mi carrera académica un buen ejemplo ni tampoco sabría decir cómo he podido (y puedo actualmente) desarrollar una carrera profesional completa sin haber cerrado un estudio superior, sobre todo en España. Si algo puedo sacar en claro después de tanto tiempo, es que mi decisión de irme fuera de España, a través de la beca Erasmus, y aprovecharla lo máximo me proporcionó herramientas que fueron y siguen siendo muy necesarias para el ingeniero de hoy día, los idiomas, la empatía hacia culturas diferentes y la curiosidad por lo desconocido.

Mi agradecimiento a todas las personas que me apoyaron siempre para poder seguir mi camino académico tan desviado del itinerario estándar. Mis padres, que sin ellos ninguna aventura extranjera o no extranjera hubiera sido posible. Que tan importante es tener una familia que apoye todas tus ideas, aunque vayan contracorriente. A mis amigos, que siempre estuvieron ahí en las buenas y en las malas en todos los momentos vividos.

Mi agradecimiento obviamente hacia todos mis mentores, grandes olvidados en el desarrollo de los profesionales de hoy día y que yo tuve la suerte de tener, sin ellos no sería el ingeniero que me considero que soy hoy, además de mucha mejor persona, mentores a los que tanto les agradeceré siempre, a Luis, Pablo, Inma, Manuel, Jordi, Jorge, Gema, Mónica, Matthias, Marion, Pachi. Siempre he tenido la suerte de poder elegir un trabajo en el que las personas que me rodean son excepcionales.

Y mi agradecimiento a mi mujer, Belén, que justo nos conocimos empezando yo este trabajo fin de grado y justo ahora que lo termino, somos una familia. Que gran paciencia y confianza ciega deposita ella en mí, nunca habrá alguien más agradecido que yo de tenerla en mi vida, una persona que no se cansa de luchar nunca, cuanta gente así hace falta en los tiempos que vivimos. Sin más, muchas gracias a todos los que me habéis acompañado de un modo u otro. Se os quiere,

Alejandro Llorente Carrión

Sevilla, 2020

Resumen

El objetivo de este trabajo fin de grado es resumir los procedimientos, métodos y equipos de última generación que se utilizan hoy en día para medir la reflectancia de un espejo en un campo solar de una planta de generación eléctrica. Aunque esa parte sólo cubre aproximadamente el 20% del trabajo, creo firmemente que, para poder hacer un resumen de un estado del arte, es necesario también revisar las bases de este. Por esa razón, el trabajo de investigación ha sido extenso y trata de cubrir la mayoría de los documentos e informes publicados desde la década de 1970 hasta el momento de publicación de este. Se han revisado casi 80 referencias y tal vez algunas de las conclusiones y declaraciones del trabajo podrían entrar en conflicto con el paradigma actual.

Este trabajo fin de grado está dirigido a los operadores de plantas que deseen tener una comprensión más profunda de todos los aspectos relacionados con la medición de la reflectancia de los espejos en un campo solar.

El trabajo de investigación ha sido extenso y trata de cubrir la mayoría de los documentos e informes publicados desde la década de 1970 hasta el momento de la redacción.

Además, los fabricantes de reflectores y sus nuevos productos han sido revisados en esta tesis para dar una visión actual del estado del arte de esta tecnología.

Tuve la oportunidad de trabajar fabricando absorbedores solares para plantas con colectores cilindro-parabólicos en una empresa alemana desde 2009 hasta 2015. Por esa razón, tengo un profundo conocimiento de la tecnología de la energía solar de concentración y mi experiencia en un entorno de fabricación intenta dar al trabajo una visión práctica de cómo implementar correctamente la medición de la reflectancia en una planta de energía solar de concentración.

Esta tesis de licenciatura ha sido escrita por un novato para principiantes en esta materia con la intención de aprender (yo primero) más sobre cómo la radiación solar llega a la Tierra, cómo se puede "cultivar" para generar electricidad y cómo todos estos pequeños defectos en los espejos, en el colector, en los cimientos, en los sensores, etc. influyen en el rendimiento de las plantas de energía solar térmica de concentración.

Este trabajo está organizado de la siguiente manera. En primer lugar, se presentan y explican los principales conceptos y terminología relacionados con la radiación solar y la medición de la reflectancia. A continuación, se ofrece una descripción detallada de los espejos utilizados en las tecnologías solares de concentración, junto con los principales factores que afectan a la pérdida de reflectancia en un espejo. A continuación, se presentarán las técnicas y dispositivos más comunes utilizados para medir la reflectancia solar tanto en el laboratorio como en el campo solar. En ese capítulo, también se centrará en cómo calcular la reflectancia solar media de un campo solar.

Como conclusión, se da una lista de mejores prácticas y de la documentación de referencia para medir correctamente la reflectancia de un espejo en una planta solar concentrada.

Este trabajo fin de grado está escrito en inglés en su totalidad y ha sido terminado en diciembre de 2020.

Abstract

The goal of this Bachelor's thesis is to resume the state-of-the-art procedures, methods, and equipment used nowadays to measure the reflectance of a mirror in a solar field. Although that part only covers roughly 20% of the work, I strongly think that for giving a picture of how it is best to do something, lying the foundations is very important. For that reason, the research work has been extensive and tries to cover most of the papers and reports published from the 1970s to the time of writing. Around 90 references have been revised and maybe some of the conclusions and statements in the work could conflict with the current paradigm. I have tried to state in the work the most updated research and developments.

This Bachelor's thesis is addressed to plant operators who are willing to have a deeper understanding of all aspects related to the measurement of the reflectance in a solar field.

Besides, the manufacturers of reflectometers and their new products have been reviewed in this thesis to give a current vision of the state of the art of this technology.

I have been manufacturing solar absorbers for parabolic troughs in a German company from 2009 to 2015. For that reason, I have a piece of deep knowledge in Concentrating Solar Power technology and my background in a manufacturing environment gives the thesis a practical vision of how to correctly implement the measurement of reflectance in a concentrated solar energy plant.

This Bachelor's thesis has been written by a newbie for newbies on such matter with the intention of learning (myself first) more about how the solar radiation reaches the Earth, how it can be "farmed" to generate electricity, and how all these tiny littles defects on the mirrors, on the collector, on the foundation, on the sensors, etc. influence the performance of the Solar Thermal Energy plants.

This work is organized as follows. First, the main concepts and terminology related to the reflectance measurement are presented and explained. Next, a detailed description of the mirrors used in concentrated solar technologies is given together along with the main factors affecting the loss of reflectance in a mirror. Following that, it will be presented the most common techniques and devices used to measure solar reflectance at the laboratory as well as at the solar field. In that chapter, it will be also focused on how to calculate the mean solar reflectance of a solar field. As a conclusion, a list of best practices and state-of-the-art references are given for measuring properly the reflectance of a mirror in a concentrated solar plant.

This Bachelor's thesis has been redacted in English and it has been finished in December 2020.

Index

LIST OF TABLES

LIST OF FIGURES

1 INTRODUCTION

The violence that exists in the human heart is also manifest in the symptoms of illness that we see in the Earth, the water, the air and in living things

- Pope Francisco -

First model for prediction of the oil production peak was published by Marion King Hubbert in 1956 [1]. After almost 65 years after the publication of Hubbert's work, the fact that the peak of the world oil production has already happened is a proven fact, supported by several publications and public data [2]. One of the main facts that support the peak oil theory is that the expected investment in fossil fuel energy in 2020 in comparison with 2019 is going to be about 18% less, according to the last World Energy Outlook 2019 [3] and if compared with 2014 data from the same agency, the drop in investment is close to 50%.

Figure 2.1 ▷ Key estimated energy demand, CO_2 emissions and investment indicators, 2020 relative to 2019

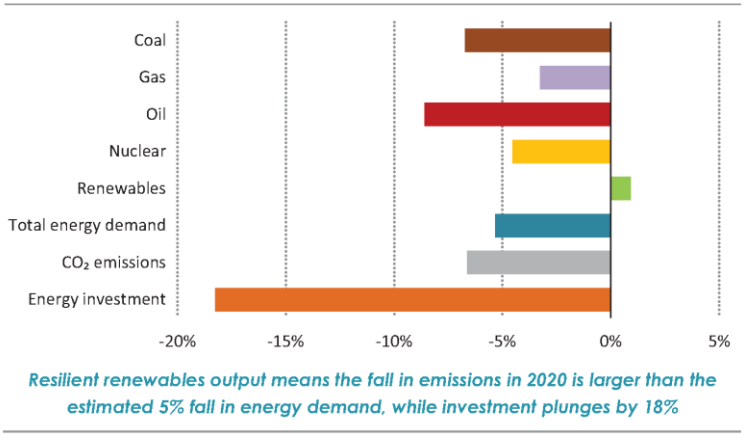

Figure 1-1 World Energy Outlook 2019, IEA, Key estimated energy demand

Therefore, the race to replace fossil technology with greener ones has taken a large share of global infrastructure and R&D investment in the last years.

One of the main participants in this race is solar technology. Solar energy is called to be a substitute for fossil fuels in the next years. More energy from sunlight strikes the Earth in 1 h (6.3×10^{20} J) than all the energy consumed on the planet in a year (4.727×10^{20} J in 2008 [4]). Although around 50% of this energy reaches the Earth's surface [5], it is only technological constraints that prevent us from exploiting its full potential.

Among this technology, Concentrated Solar Power (CSP) plays a big role in this change. Despite annual CSP capacity addition in the world in 2019 is only 0.60% of the total PV capacity addition [6], in the last 9 years, the concentrated solar technology has reduced its Levelized Cost of Electricity (LCOE) by almost a 50% according to the International Renewable Energy Agency (IRENA) last published data. (From an average 0.3460 $/kWh in 2010 to 0.1820 $/kWh in 2019. Lazard asset management firm established the 2020 CSP averaged LCOE in the range 0.126 - 0.156 $/kWh[1] [2]). See Figure 1-2.

[1] Data in the IRENA Auction and PPA Database shows a weighted-average price of electricity of 0.075 $/kWh for CSP projects to be commissioned in 2021. This represents a reduction of 59% when compared to the global weighted-average project LCOE in 2019. https://www.irena.org/Statistics/View-Data-by-Topic/Costs/Global-LCOE-and-Auction-values

[2] Morocco's 800 MW CSP-PV Noor Midelt breaks last year's auction price record of 7.3 cents set by DEWA in the UAE, with winning bid at USD 7 cents/kWh. So, the LCOE of such CSP installations is less than the last averaged range 0.126 - 0.156 $/kWh stated by Lazard's. Source: https://www.solarpaces.org/morocco-breaks-new-record-with-800-mw-midelt-1-csp-pv-at-7-cents

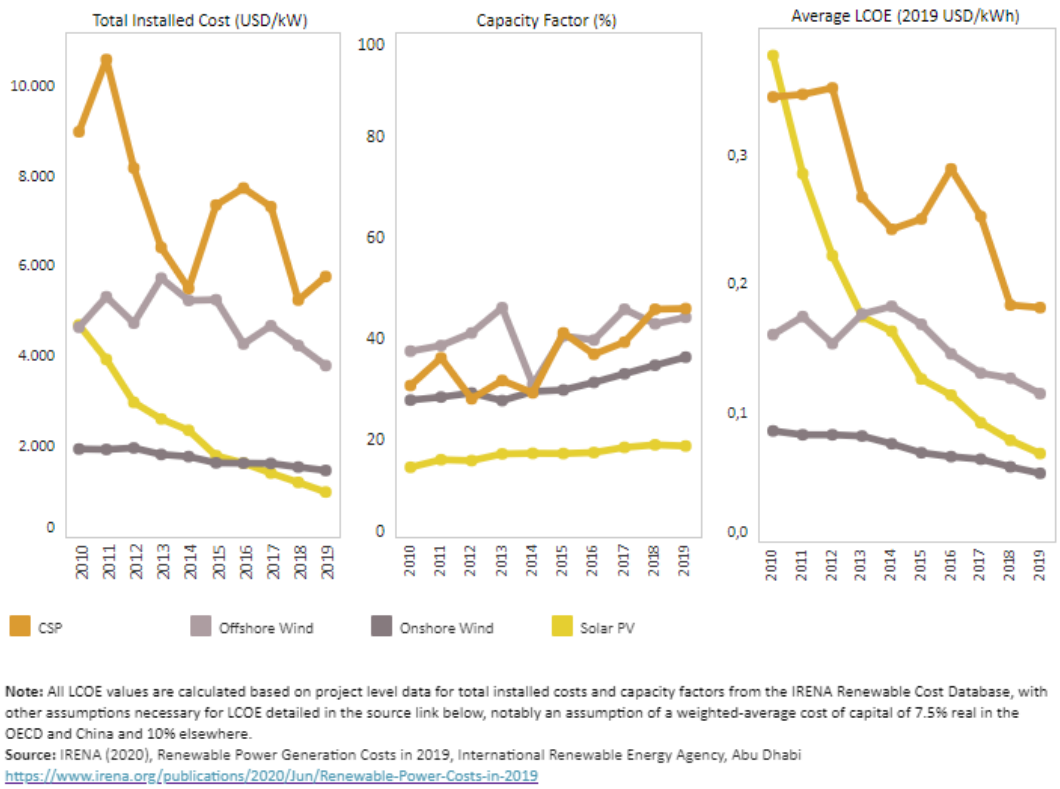

Note: All LCOE values are calculated based on project level data for total installed costs and capacity factors from the IRENA Renewable Cost Database, with other assumptions necessary for LCOE detailed in the source link below, notably an assumption of a weighted-average cost of capital of 7.5% real in the OECD and China and 10% elsewhere.
Source: IRENA (2020), Renewable Power Generation Costs in 2019, International Renewable Energy Agency, Abu Dhabi
https://www.irena.org/publications/2020/Jun/Renewable-Power-Costs-in-2019

Figure 1-2 IRENA 2020, CSP, Renewable Power Generation Costs in 2019

The CSP technology offers a better Capacity Factor than Solar PV, 45% versus 18% of the latter [7] [8], with only 1% of the global installed capacity concerning solar PV [9]. Then offering a more stable and reliable energy generation, making this type of technology like that generated by fossil fuels, dispatchable, and predictable. It is common to compare generation technologies using as Key Performance Indicators (KPI) the LCOE, or the capital costs [$-€/MW], but the dispatchability and predictability of a generation technology are far more important in countries like Spain, where the generation curve is not flat but has two pikes during the day, at dawn and evening. In such countries, fast-ramping generation technologies like the CSP with energy storage gives this technology an advantage against its greener competitors, solar PV, and wind. While CSP technology is still expensive in capital costs and operating costs than the solar PV or wind technology, when talking to system level, the value of the overall investment shall be considered: dispatchability, accountability, components performance degradation, grid stability, distributed vs centralized generation or maturity of the technology are, among other important factors, indicators to better assess the suitability and value of renewable generation technology.

Nor the power installed, or the energy generated by different sources have the same value in Spain or Germany, or California, it is dependent on the grid and electrical system in which this energy is feeding in. Two terms describe better the value of the generated electricity: operational value mean and capacity value mean. The operational value represents the avoided costs of conventional generation at their respective dispatching times along with related ancillary services costs, such as spinning reserve, etc. Savings on emission costs are also accounted for. Capacity value reflects the ability to avoid the costs of building new conventional generation in

response to growing energy demands or plant retirements. One of the most accurate studies about the value of CSP was done by NREL [10] demonstrating that the value of CSP plants to the electrical system in California is double that of PV in a scenario of 33% penetration of renewables when operational and capacity value for the system of new plants are duly considered. The value will be triple in a 40% renewable penetration scenario. As an example of an advantage of having connected a CSP plant into the main grid, they can store energy in Thermal Energy Systems (TES), feeding this stored energy to the main grid when the electricity is needed due to demand.

CSP plant developers were the pioneers to increase the dispatchability of such Solar Thermal Energy (STE) plants. Beginning 2000s, Battery Energy Storage System (BESS) were still too expensive for use in large scale utility plants (CAPEX BESS 1500 $/kWh vs TES 50 $/kWh), so CSP contractors industrialize the energy storage using molten salt as a medium in where to save process heat. Using solar energy as a resource, the CSP plants were the only ones able to produce energy once the sun had gone down, saving heat in molten salt tanks in the daylight and using it during the night to maintain nominal steam temperatures for at least 7.5 hours, as it is in the Andasol Solar Power Station, first parabolic trough power plant in Europe [11].

In any solar concentrating technology, from the most maturity ones like parabolic-trough collectors (PTC) or solar tower (ST) with molten salt TES to the newest concepts like fallen particle receivers, molten salt direct storage, or solar fuels, mirrors are present to focus the direct solar radiation into a receiver and increase the solar flux. In a typical solar power plant of 50 MWe like the PTC plant of Andasol in Spain, mirrors are responsible for almost 8% of the total investment in a concentrated solar power plant. The solar field itself represents the bigger part of the CAPEX in a PTC or ST plant, see Table 1-1.

Table 1-1 CSP plant cost breakdown, 2019 (Crespo, 2021)

150MW with 9h Storage	Parabolic-Trough (%)	Solar Tower (%)
Solar field	42	30
Tower and receiver		12
HTF system	10	7
Storage system	13	10
Power block	17	19
Control system	4	5
Electrical system	5	6
Auxiliary systems	5	5

150MW with 9h Storage	Parabolic-Trough (%)	Solar Tower (%)
Site and project development	4	6

As stated before, for this technology to match costs and benefits with the other greener competitors even with the fossil fuel ones, it needs to increase efficiency and reduce the technology costs, specifically mirrors. For that reason, having well-proven protocols, accurate plant models and reliable measurement equipment is critical for reaching a low OPEX in such STE plants.

The key functionality of a mirror is to reflect the light as specular and efficient as possible to the solar collector. From the point of view of the operator, to measure the performance of a solar field, a standard procedure that minimizes the time consumed in such tasks will help optimizing plant costs. Such a procedure must reduce uncertainty and complexity in characterizing a mirror reflecting beam and help to predict its behaviour over time. On the other hand, portable or in real-time measurement devices must be developed in a cost-efficient way to make state-of-the-art technology to be in use in the field. Therefore, to cut capital and operational costs of a solar field, developing operational-proven characterizing standards and accurate measuring devices will help to better assess the performance of a mirror and will give the operator information valuable information about its cleanliness, aging status, or structural condition.

In this Bachelor thesis, both procedures and equipment that can measure reflectance are discussed, to get an overview of the differences and challenges that exist between the laboratory and the field.

As a simple approach, a 5 Ws and How (5W1H) problem-solving procedure could be used to help a CSP operator in the task of measuring the mean reflectance of a solar field. Who and Why can be neglected from the equation, but the other whys and how questions must be answered to make better decisions for the optimal operations of the plant: What properties must be measured? When must they be measured? Which mirror or location of the mirror must be measured and most important, how must they be measured? This thesis will try to answer these questions or at least, will point to the reference in which to find them.

Studies about the characterization of the solar reflectance spectrum date back to 1976 with Richard B. Pettit and its work about “Characterization of the reflected solar beam profile of solar mirror materials” [12]. The work done by Pettit et.al. is still valid today and should be taken into consideration by any plant operator because it found the influence of dust over the mirror surface and the scattering producing by it [13].

The knowledge of reflectance measurement and all its involved factors has been always a matter of study since the 1980s. However, there are still challenges about how to measure the solar field mean reflectance with low uncertainty and without the need to measure it locally on the field by an operator.

There are international standards and guidelines establishing the state-of-the-art procedures to evaluate the reflectance properties of a reflective material such as the published from the Task III group within the Solar PACES organization [14] or the UNE Standard 206016:2018. [15].

The SolarPACES, founded in 1977, is an "international network of researchers, under the IEA Technology Collaboration Programme, leading the technology development, market deployment and energy partnerships for sustainable, reliable, efficient and cost-competitive concentrating solar technologies" [16]. Currently, as far as concentrating solar power technology is concerned, the SolarPACES task groups are the reference for developments and research activities related to concentrating solar power. To this work, the SolarPACES task III: Solar Technology and Advanced Applications is the reference.

The mirror reflectance could be influenced by many factors, many of them not measurable by a single piece of equipment. The data calculated by a device must be treated accordingly to the case of the study (mirror type, concentrator, site location, etc). Due to the variety of locations of concentrated solar energy plants worldwide, it might be that a standard or procedure valid for a plant located in Spain could not be valid or give inaccurate information for a plant located in Morocco [17]. This is true because the soiling type and rate are different and, consequently, the frequency and number of measurements required could vary [18]. Thus, the information needed to obtain a reliable measure of the mirror reflectance value could be greater or lesser depending on where the solar field is located on the Earth.

This thesis will collect most of the current procedures on how to calculate the solar mean reflectance of a solar field in a CSP plant and the most common and last measurement devices used in present plants.

2 CONCENTRATED SOLAR POWER. WORLDWIDE AND SPANISH CURRENT STATUS

Concentrating solar power (CSP) systems use combinations of mirrors or lenses to concentrate direct beam solar radiation to produce forms of useful energy such as heat, electricity, or fuels by various downstream technologies.

Within the concentrating solar power plants, there are several categories to describe them, as can be seen in Table 2-1:

Table 2-1 Concentrating Solar Power Plants Categories

Based on the heat transfer fluid: • Water • Air • Oil • Molten salt • Dispersed particles	Based on the geometrical focus: • line focus (1D) • point focus (0D)
Based on the technology • Linear Fresnel Reflector • Parabolic-Trough Collector • Solar Tower • Parabolic Dish • Solar Furnace	Based on its thermodynamic cycle: • Stirling • Rankine • Brayton
Based on the receiver type • Fixed • Mobile	Based on how the reflector concentrates the reflected light: • Imaging concentrator • Non-Imaging concentrator

Despite the number of different technologies and classifications, the PTC with oil as heat transfer fluid is the most used by far for utility-scale generation plants [19], see Table 2-2.

Table 2-2 World CSP installed electrical capacity (Protermosolar, 2020)

Type of Technology	World CSP Installed Capacity (%)	World CSP Installed Capacity (MWe)
PTC	74.80%	4604.1
ST-Steam	9.41%	579.01
ST-Molten Salt	8.12%	499.9
PTC-ISCC	2.88%	177
LFR	2.28%	140.4
PTC-Molten Salt	1.71%	105
LFR-Molten Salt	0.81%	50

In the coming future, Central Receiver Systems (tower systems mostly) seems to be taking the advantage as the leading technology in this field, as its capacity under development for new projects double the developed for PTCs, see Figure 2-1.

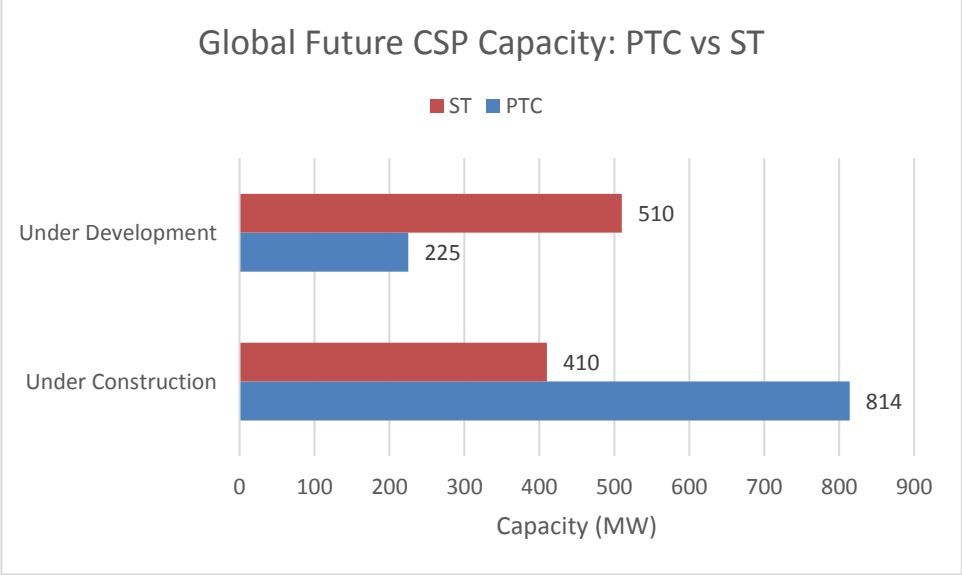

Figure 2-1 Global Future CSP Capacity: PT vs CRS (Protermosolar, 2020 [3])

At the beginning of 2020, there were 6155 MWe installed in the world, most of them installed in Spain (2304 MWe) and the USA (1694 MWe). However, the economic crisis of 2012 in Spain brought the investment in solar thermal energy plants to an abrupt halt. Feed-in-tariff incentives were withdrawn for this kind of technology and the installation of new renewable capacity stopped. No STE plants have been connected to the grid since 2013 due to this situation. 2019 CSP quota concerning all renewable energies in Spanish installed capacity is

[3] Dataset from the website https://www.protermosolar.com/proyectos-termosolares/proyectos-en-el-exterior. Recently the SolarPACES organization has published a database with metadata of concentrating solar power plants of the world for energy modellers and analysts, https://csp.guru/

5.3 %.

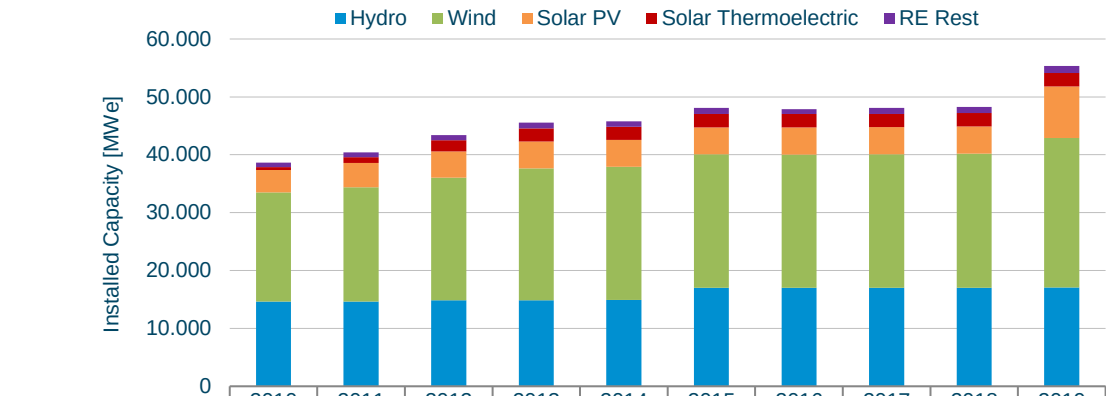

	2010	2011	2012	2013	2014	2015	2016	2017	2018	2019
RE Rest	782	820	886	972	948	1.054	872	1.044	1.048	1.248
Solar Thermoelectric	532	999	1.950	2.299	2.299	2.304	2.304	2.304	2.304	2.304
Solar PV	3.829	4.233	4.532	4.638	4.646	4.678	4.683	4.685	4.712	8.913
Wind	18.861	19.707	21.167	22.758	23.009	23.028	23.004	23.050	23.130	25.799
Hydro	14.656	14.668	14.887	14.890	14.897	17.026	17.030	17.028	17.046	17.085

Figure 2-2 Cumulative renewables installed capacity in Spain from 2010-2019 (REE, 2020)

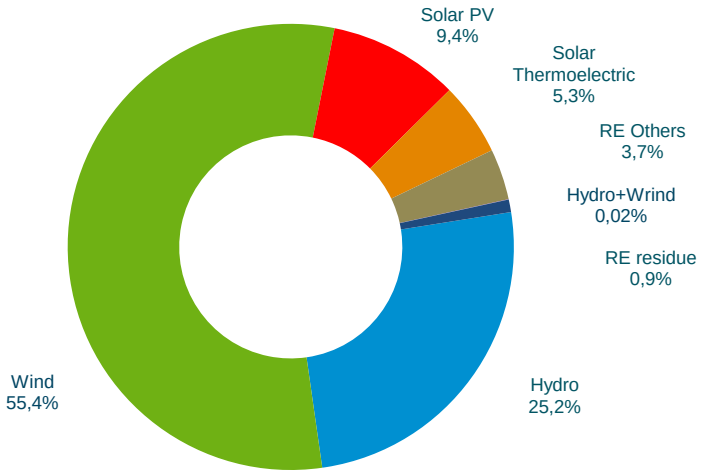

Figure 2-3 Renewable installed capacity distribution in 2019 (REE, 2020)

CSP market for new installations has moved to Morocco, South Africa, and Saudi Arabia mostly, with China and Chile participating actively. China and Chile will be the only countries to connect CSP STE plants to their grids in 2020 (Protermoslar, NREL), see Figure 2-4.

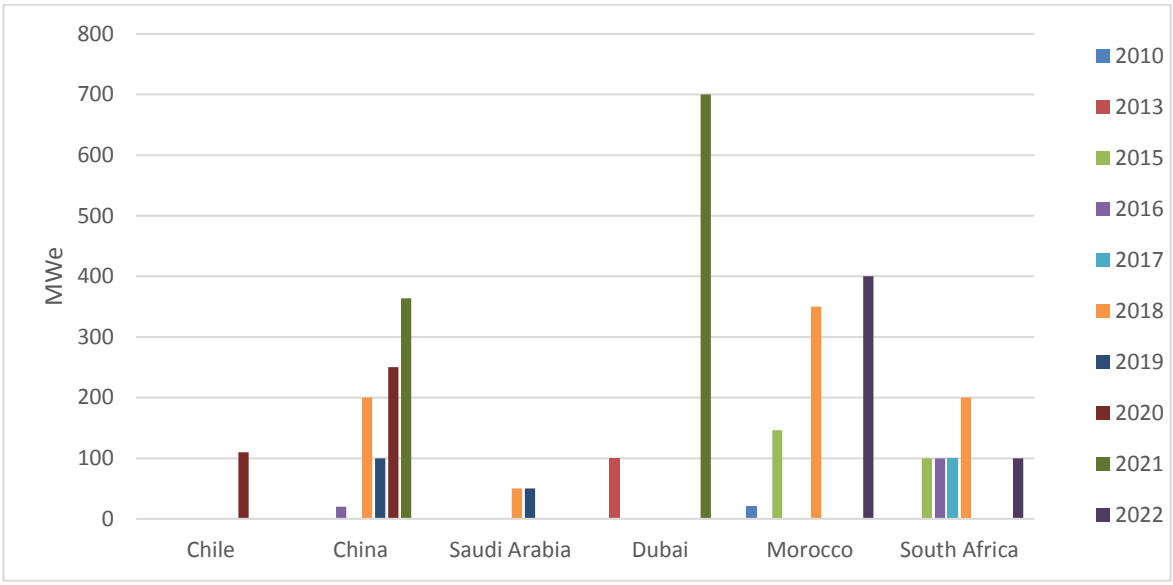

Figure 2-4 CSP new markets. Installed, in construction and in-development capacity (Protermosolar, 2020)

For new plants, the trend in utility-scales is PTC plants with more than 8 hours in storage, but every year more CRS plants are being installed in the world, as can be depicted in Figure 2-5.

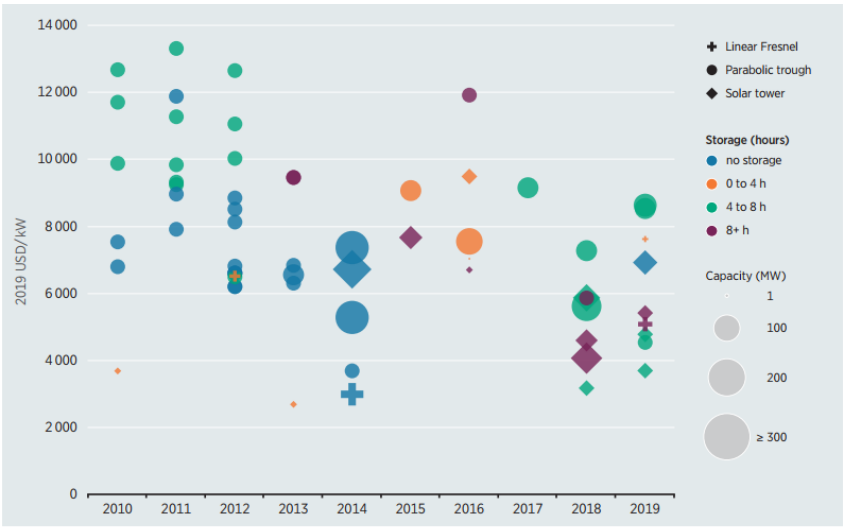

Source: IRENA Renewable Cost Database.

Figure 2-5 CSP total installed costs by project size, collector type, and amount of storage, 2010-2019

Electricity costs from renewables have fallen sharply over the past decade, as a result, in 2019, 72% of all new capacity additions worldwide has come from renewable technologies [7]. Installation of new renewable capacity in the world is growing at an 8.4% rate averaged for the last 9 years.

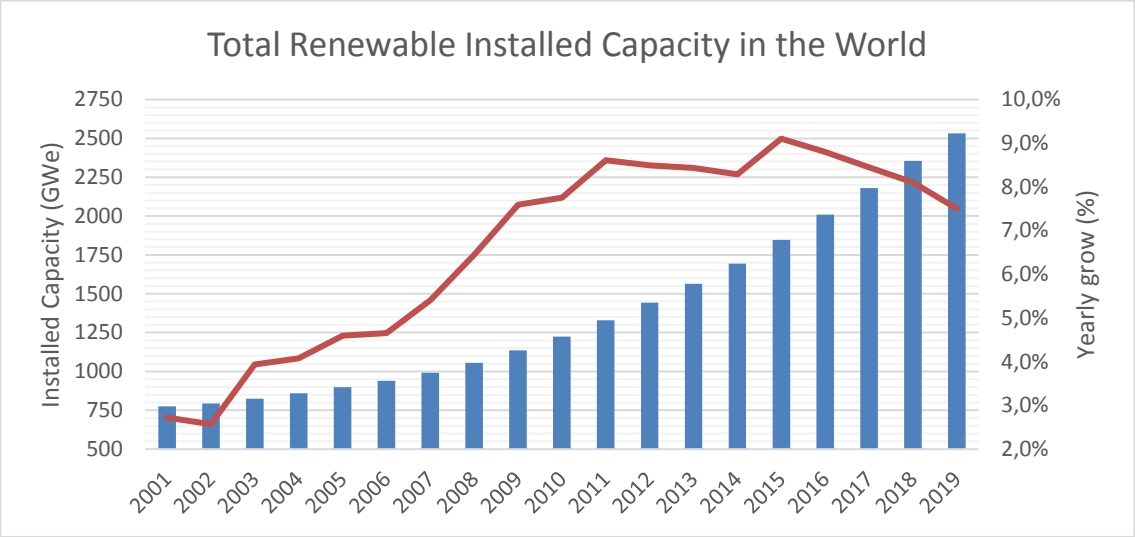

Figure 2-6 Total of renewable installed capacity (GWe). Sources: IRENA and UN statistic database [20]

While the addition of new capacity coming from non-renewable sources grows at a very flat rate (0.2%-0.4% averaged from 2010-2017) [20]. This constant increase in investment and massive deployment of renewable infrastructure has as a result that most of the renewable mature technologies have a weighted-average LCOE in range with the fossil fuel cost, see Figure 2-7.

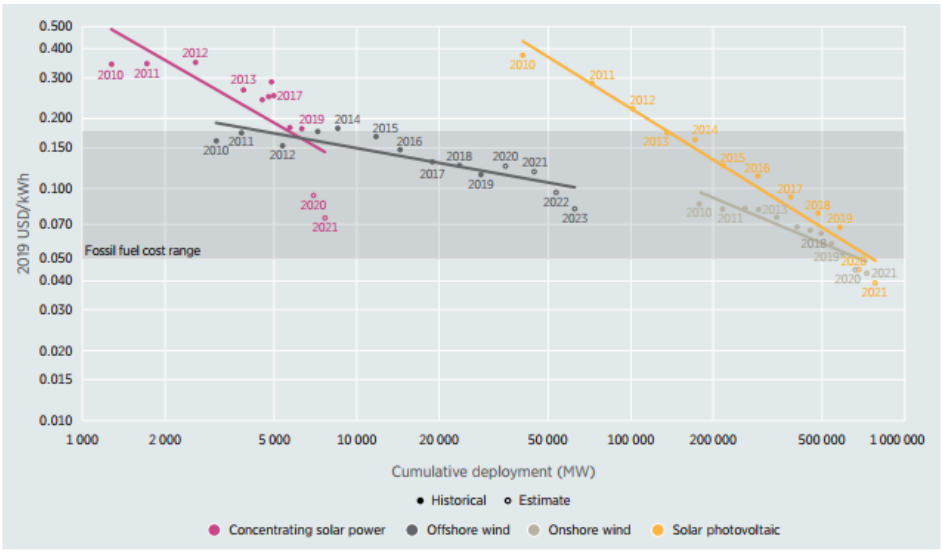

Source: IRENA.
Note: The LCOE and auction price data are for utility-scale projects.

Figure 2-7 The global weighted-average LCOE and Auction/PPA price learning curve trends for solar PV, CSP, onshore and offshore wind, 2010-2021/23

It is a fact, that in the advanced economies, the continuously growing penetration of intermittent electricity sources will increase the future demand for dispatchable power plants, which balance out fluctuations within the electrical grids. Intermittent generation of electricity has not been always easy to handle and to optimise for most of the grid operators. Searching for a more stable, reliable, and optimised grid is always the main mission of any

grid regulator, so the increase of renewable energy in the generation mix could become a problem in the coming years if this trend stays continues. For that reason, hybridization projects in which renewable sources not only generate electricity but also reduce other fossil fuel consumption activities could be beneficial. In that role, CSP plants play a big part. CSP usually produces heat as an intermediate process, so this process heat might be used for thermally-driven industrial processes like enhanced oil recovering, desalination, agriculture and food processing, ramp-up for turbines in Integrated Solar Combined Cycle Power Plants (ISCC), drying sludge for water treatment, mid-pressure steam, or the last trendy initiatives like hydrogen reforming, making this kind of technology suitable for not only generate electricity but for substitution fossil fuel activities in large factories or industrial processes, for a more detailed statement of the long-term market potential of CSP systems, please refer to [21].

Having summarized the pros and contras of such technology, the next chapter will focus on understanding the main characteristics of solar radiation reaching a mirror.

3 SOLAR REFLECTANCE. THEORETICAL BACKGROUND

In this chapter, it will be summarized the most important concepts involving the calculation of the solar reflectance.

3.1 Solar radiation terms

To better understand how to focus the solar radiation on an absorber surface, this section will describe how the sunbeams reach the Earth's surface and its main characteristics.

3.1.1 Solar constant or Total Solar Irradiance (TSI)

To understand how to concentrate the light in a line or a point is essential to understand how the sunlight is delivered to the earth and the main parameters which define this transport of photons.

For that purpose, the concept of solar constant G_{SC} defines the total radiative flux at all wavelengths incident on a surface normal to the sun rays at a distance of 1 Astronomical Unit (AU).

The radiation intensity on the surface of the sun is approximately 6.33e10^7 W/m^2. Since radiation spreads out as the distance squared, by the time it travels to the earth, the radiant energy falling on 1 m^2 of a surface area is reduced to approximately G_{SC} = 1360.8 W/m^2 ± 0.0005 W/m^2 [22] outside the earth's atmosphere as depicted in Figure 3-1.

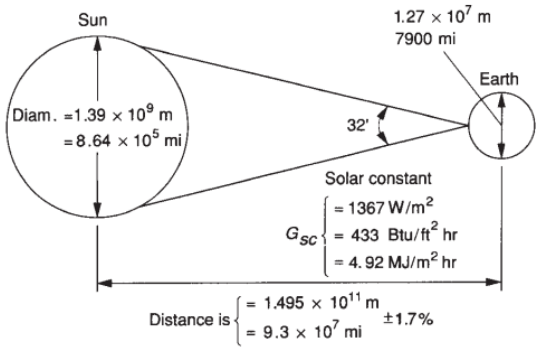

Figure 3-1 Sun-Earth relationships (Duffie, 2020)

The distance between the sun and the earth changes by ± 1.7 % between apogee and perigee. This affects the value of the total solar irradiance depending on the time of the year, so the $G_{0,n}$ could be calculated according to equation ((3-1):

$$G_{0,n} = \left[1 + 0.033\ cos\left(\frac{360^o \cdot n}{365.25}\right)\right] G_{SC} \quad (3\text{-}1)$$

Where n is the day of the year after 1 January and G_{SC} is the solar constant [23].

3.1.2 Sunshape and sun's beam deviation (angular width of the sun)

The brightness of the Sun's disc is not perfectly uniform. When viewed from the Earth, the Sun appears as a disk with an angular radius of 4.65 mrad (see Figure 3-2). All the radiation incoming from 4.65 mrad to 50 mrad in a collector is what is called circumsolar radiation (Rabl and Bendt, [24]). Angular radius larger than 50 mrad is considered diffuse radiation.

The circumsolar radiation is the radiation coming from the adjacent region around the sun. The actual sun shape is most strongly influenced by prevailing atmospheric conditions, particularly the level of particulate matter or moisture in the sky. The circumsolar radiation does not include backscattering from the other sources.

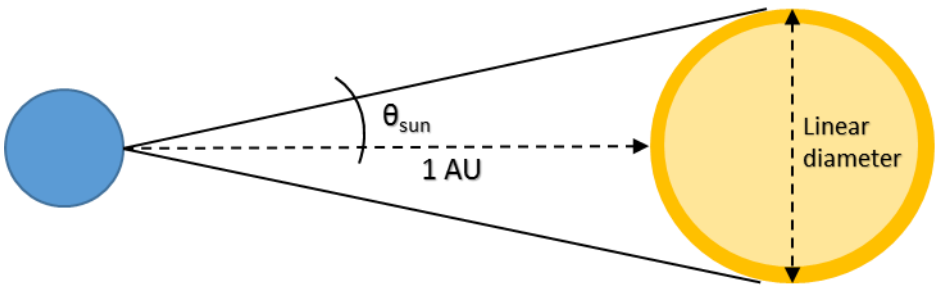

Figure 3-2 Angular shape of the sun viewed from the Earth

The solar radiance is a function of the subtended angle θ_{sun} measured from the centre of the sun. Sunshape data are typically presented in terms of the radiance distribution $B(\theta_{sun})$, which has the units (W/m^2 sr). θ_{sun} is a solid angle. Bendt and Rabl measured the standard solar brightness distribution $B(\theta_{incidence})$ as can be seen in figure 3-3.

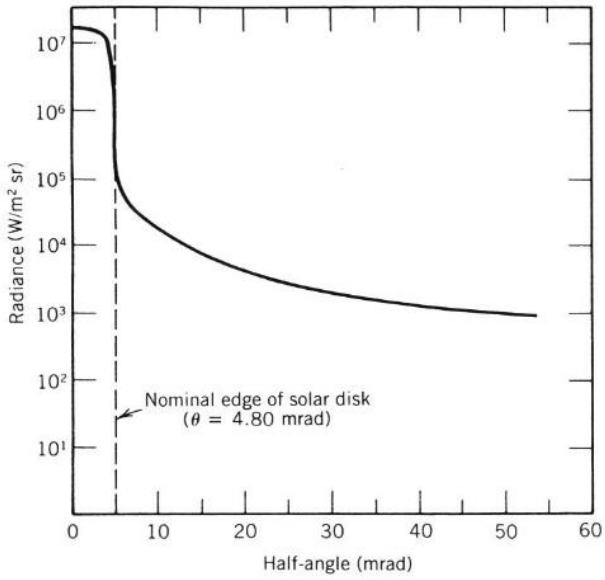

Figure 3-3 Radiance distribution $B(\theta_{incidence})$ of a "standard" solar scan showing both solar disc and circumsolar radiation (Bendt and Rabl, 1980)

Being the angular spread of the sun reaching the earth (half-angle) θ_{sun} = 4.65 mrad, there is a physical limit to the concentration of solar radiation. The second law of thermodynamics requires that the maximum possible concentration for a given acceptance half-angle θ for two-dimensional concentrators like the PTC is [23]:

$$C_{ideal.2D} = \frac{1}{\sin \theta_{sun}} \approx 215 \tag{3-2}$$

This concentration ratio is ideal, the concentrator systems must be designed with an acceptance angle larger than the angular spread of the sun due to several reasons like non-ideal reflectors, receiver misalignment, scattered incoming radiation, etc. The larger the acceptance angle of a collector, the more diffuse solar radiation it might reflect, but for collectors with concentration ratios larger than 10, the diffuse radiation collected might be neglectable [23]. The sources of loss performance in a collector will be treated in chapter 5.2.

3.1.3 Air Mass for solar purposes

The Air Mass (AM) describes the path length of the solar radiation through the atmosphere. The relative air mass is defined in the equation (3-3):

$$AM = \frac{L}{L_0} \approx \frac{1}{cos(\theta_z)} \tag{3-3}$$

Where L is the path length through the atmosphere, L_0 is the height of the atmosphere and θ_z is the solar zenith angle, relative to the normal to the Earth's surface, as can be seen in Figure 3-4. Figure 3-5 shows various AM cases depending on the solar zenith angle θ_z.

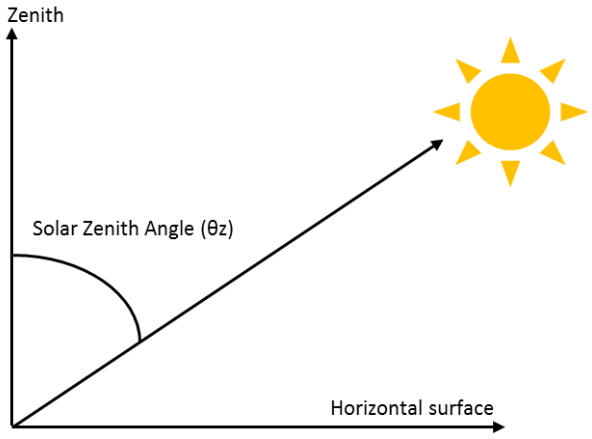

Figure 3-4 Zenith angle definition

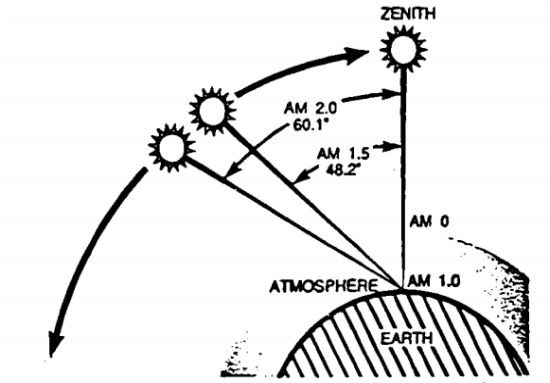

Figure 3-5 Air Mass examples (Oriel Corporation, 1994)

The sunlight passing throughout the atmosphere is attenuated by aerosol scattering and by absorption caused by aerosols and gasses such as CO_2, H_2O (attenuates in the IR-range), and O_3 (attenuates in the UV-range) mainly, see Table 3-1.

Table 3-1 Absorption and scattering for typical clear-sky conditions (Vignola et al., 2012)

Factor	% absorbed	% scattered	% of total passing through the atmosphere
Ozone	2	0	
Water vapour	8	4	
Dry air	2	7	
Aerosol	2	3	
Total not absorbed or scattered	≈ 87	≈ 87	≈ 76

The attenuation of solar radiation by the atmosphere is not the same for all wavelengths, hence the importance

of using the correct AM spectrum when calculating reflectance using a solar spectral irradiance standard like the ASTM G173-03 (2020) [25]. For applications using direct solar radiation, the AM 1.5D spectrum is used to find the specular solar reflectance, which is the solar radiation solar concentrators used in power generation.

3.1.3.1 Clearness Index (K_T)

To identify the feasibility of solar energy utilization and predict the solar average irradiation there are several parameters in the bibliography to be taken into account, but the clearness index (see equation (3-4)) gives a fair estimation about the relationship between terrestrial and extraterrestrial insolation over a horizontal surface:

$$K_T = \frac{H_h}{H_o} \tag{3-4}$$

Where H_h is the horizontal global irradiation and H_o is the extraterrestrial irradiation on a horizontal surface. The clearness index can also be defined using irradiance instead of irradiation. On cloudy days K_T may be as low as 0.05 - 0.1 while on clear days it is in the range of 0.7 - 0.8. Monthly averages of K_T range from 0.4 for very cloudy climates to 0.7 for very sunny climates. As shown by Angstrom [26], the monthly average clearness index K_T is closely correlated with the monthly average number of sunshine hours. For a more accurate definition of this term, the reader can be directed to [26]. The monthly average clearness index for various locations around the world can be found in the Homer Energy website [27] or the NASA prediction of worldwide energy resources [28].

The clearness index, K_T, is not to be confused with the cleanliness factor, F_C, used in the STE plants to measure the soiling ratio in the heliostat field. This will be described in chapter 5.2.

3.1.4 Global Horizontal Irradiance, Diffuse Horizontal Irradiance, and Direct Normal Irradiance

The Global Horizontal Irradiance (GHI) is the sum of direct and diffuse radiation received per unit from a solid angle 2π stereoradian (sr) on a horizontal plane. GHI is the reference radiation for the comparison of climatic zones.

The Diffuse Horizontal Irradiance (DHI) is the amount of radiation received per unit area by a surface (not subject to any shade or shadow) that does not arrive on a direct path from the sun but has been scattered by molecules and particles in the atmosphere and comes from all directions.

The Direct Normal Irradiance (DNI) is the amount of solar radiation received per unit area by a surface that is always held perpendicular (or normal) to the rays that come in a straight line from the direction of the sun at its current position in the sky.

The maximum terrestrial DNI varies significantly with location and weather conditions but is often taken as 1000 W/m2. DNI data are available in different databases typically with hourly resolution [29]. Being the θ_z the zenith angle (see 3.1.3), these three concepts are related as described in the equation (3-5):

$$GHI = DHI + DNI \cdot cos(\theta_Z) \tag{3-5}$$

As non-concentrating photovoltaic (PV) can also utilize a substantial amount of diffuse irradiance, GHI is closely related to the assessment of PV energy yields, while DNI is applied for the estimation of energy yields from CSP and CPV (concentrating PV) plants. There are some theoretical models in which they calculate the DNI through the AM coefficient and extraterrestrial radiation, see [30] for further information.

3.1.5 Spectral solar irradiance $G_b(\lambda)$

The irradiance at a point of a surface is the radiant instantaneous power of all wavelengths incident from all upward directions falling on a unit area per unit time, SI unit: W/m^2. The symbol G is used to describe the solar irradiance (insolation, radiant flux, and flux density are also synonyms in engineering terms, but they are used in different contexts).

The spectral irradiance, denoted as $G_b(\lambda)$, is the irradiance at a given wavelength per unit wavelength interval. SI unit: W/m^2/nm or W/m^2/μm. Then, the total radiant power Φ is denoted as in equation (3-6):

$$\Phi = \Phi_\lambda = \int_0^\infty \Phi_\lambda d\lambda \ \text{ SI-unit [W/m}^2\text{]} \tag{3-6}$$

The solar irradiance spectra could be divided into 3 regions: ultraviolet, visible, and near-infrared. As can be seen in figure 3-6, the visible range of the solar flux contains the most powerful energy wavelengths of the sun, so the ideal mirror must reflect primarily above the 400 nm range.

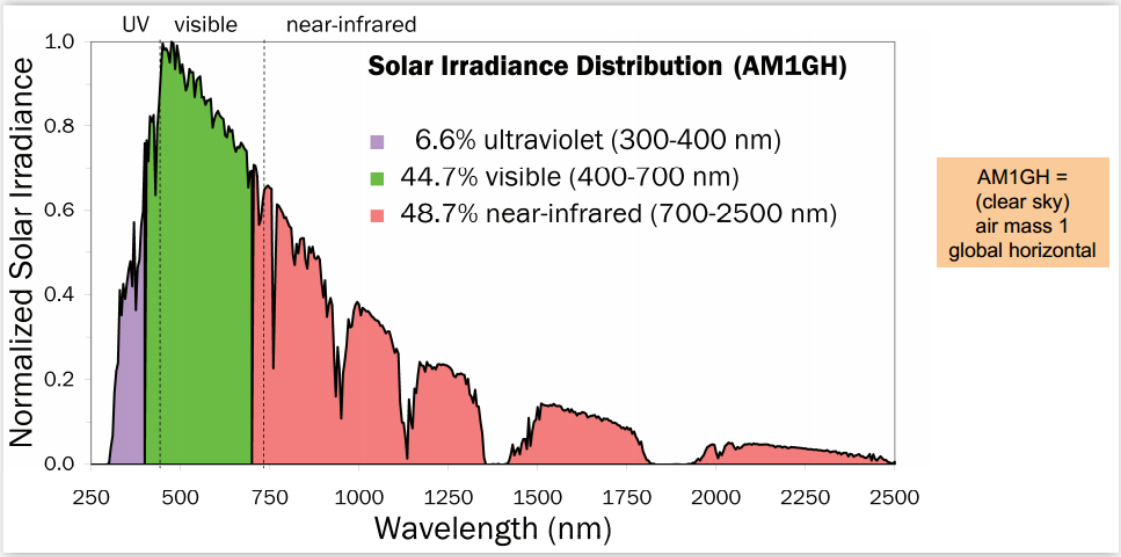

Figure 3-6 Spectral solar irradiance distribution for AM1GH spectrum

The knowledge of the relative amount of energy contained in sunlight at different wavelengths allows the engineer to evaluate the impact of wavelength phenomena on the total energy collection.

3.2 Reflectance definition and the law of reflection

The National Institute of Standards and Technology (NIST) in the United States of America (USA) defines reflectivity as an intensive property of a material, just as resistivity, thermal conductivity, etc. On the other hand, the reflectance is defined as an extensive property of a material. When talking about the optical properties of a material in solar applications, the ending "-ance" must be used, because such materials can be degraded by thermal processes, soiling, corrosion, etc. and that has an effect on their intrinsic properties [31]. From now on as far as mirrors are concerned, only the term reflectance will be used.

A mirror could reflect a light beam in different ways. It is important to define the characteristics of a reflected beam and standardize the symbols and parameters which define the reflected spectra. Hereunder a standard definition of the reflectance concept will be presented along with its classification.

The reflectivity (in this case is reflectivity because is only one layer) of a surface, ρ, according to UNE-EN ISO 9488 [32], is the "ratio of the energy flux reflected, $\Phi_{reflected}$, by a surface to the radiation incident on it, $\Phi_{incident}$", see equation (3-7).

$$\rho = \frac{\Phi_{reflected}}{\Phi_{incident}} \tag{3-7}$$

In any layer of a mirror setup must be met that the sum of absorptance, transmittance, and reflectance is equal to 1. The reflectance of a mirror is a dimensionless magnitude ranging from 0 to 1, which depends on wavelength, λ, the direction of the incident radiation or incidence angle, θ_i, direction of the reflecting radiation, θ_r, the reflecting light acceptance surface size $S(\Omega)$ and the temperature of the surface T_s. In this work, 1 reflectance units will be the same as 100 percentage points (ppt) and will be the same as 100% absolute reflectance of a reflector. The temperature of the surface (T_s) will be considered constant along in a reflectance measurement and its effects on the reflected beam will be omitted.

When a light beam impinges a material, the first law of reflection states that the incident ray, the reflected ray, and the normal to the reflective surface at the point of incidence lie in the same plane. The second law of reflection specifies that the angle of incidence, θ_i, is equal to the angle of reflection, θ_r. This last statement is true for an ideal reflector. In that case, if all the incoming light beams are reflected according to the laws of reflection, the reflectance of the mirror is called specular, $\rho_{specular}$ or ρ_{φ}. However, imperfections over the surface of a layer like roughness, particles, scratches, inhomogeneities in the chemical composition, etc. cause that the direction of the reflected irradiance is not always specular. Many light beams are scattered around the supposed ideal spatial direction, creating more diffuse (or scattered) reflectance, $\rho_{diffuse}$ or ρ_d. Therefore, in general terms, we can define the total reflectance as, ρ_{total}, see equation (3-8):

$$\rho_{total} = \rho_{specular} + \rho_{diffuse} \tag{3-8}$$

The total reflectance is also known as hemispherical reflectance, $\rho_{hemispherical}$ or ρ_h, since this one measures the reflected light regardless of its directionality. As for CSP purposes, the correct addressing of the measurement of both specular and diffuse reflectance is a key task in a solar power plant to have an overview of the general performance of a solar field and its aging condition. The solar reflectance model will be described deeper in the next sections.

3.3 Characterization of the solar reflectance: specular, diffuse, and hemispherical reflectance

The solar reflectance concept, according to UNE 206009:2013 [31], is defined as "the reflectance weighted in the solar spectrum". Since the visible range of the solar flux contains the most powerful energy wavelengths of the sun, measuring the reflectance according to its wavelength makes sense for solar concentrating applications.

In the nomenclature, the solar reflectance is indicated with the subscript *s* after the reflectance symbol, ρ_s, while the reflectance given just at a certain λ is named as monochromatic reflectance and its symbol is ρ_λ. Normally, the temperature T_s is the ambient temperature (25 ºC ± 2 ºC). The effect of this parameter in the reflectance calculation will be omitted as has been mentioned before. ρ_s expressed in general terms can be described as in equation (3-9):

$$\rho_s([\lambda_a, \lambda_b], \theta_i) = \frac{\int_{\lambda_a}^{\lambda_b} \rho_\lambda(\lambda, \theta_i) \cdot G_b(\lambda) d\lambda}{\int_{\lambda_a}^{\lambda_b} G_b(\lambda) d\lambda} \tag{3-9}$$

This definition is also known as solar-weighted reflectance. The values to be used for the solar spectral irradiance term $G_b(\lambda)$, are recommended to be taken from reference standards as the ASTM G173-03 (2012) [25], spectrum AM 1.5.

Solar-weighted specular reflectance is the most relevant parameter to assess the quality and status of the reflection by mirrors since gives not only information about which portion of the solar irradiation is being reflected but also if it is being reflected properly towards the receiver. However, as Aránzazu *et al.* [14] stated in the SolarPACES Reflectance Guidelines 3rd edition, it is not currently possible to measure the specular reflectance spectrum at a specified angle of acceptance and within the whole solar spectrum with commercial portable devices, therefore, the solar-weighted hemispherical reflectance and the monochromatic specular reflectance are the relevant and almost unique parameters to evaluate the quantity of solar irradiance reflected

in the collector.

Then, hemispherical, and specular reflectances are the most representative values of a reflector, so in the next subsections, the definition and standard nomenclature for these concepts will be presented.

3.3.1 Hemispherical reflectance

According to UNE 206009:2013 [31], the hemispherical reflectance is "the ratio of the energy flux reflected by a surface within the complete hemisphere over that surface to the radiation incident on it."

As it is depicted in Figure 3-7, the hemispherical reflectance is the collection of all reflected beams into the hemisphere above the reflecting surface of a mirror.

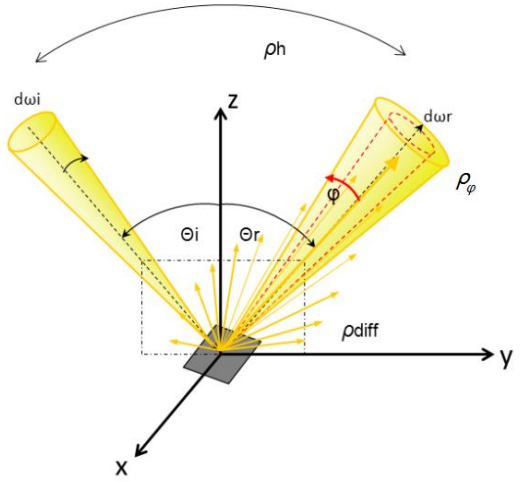

Figure 3-7 Geometry of an incident and reflected beam in a reflective material (A. Heimsath et al., 2011)

Therefore, the hemispherical reflectance is the sum of the specular reflectance and the diffuse reflectance, ρ_h. The solar hemispherical reflectance is indicated with the s (for solar) as the first subscript and the h (for hemispherical) as the second subscript, and it is defined in equation (3-10):

$$\rho_{s,h}([\lambda_a,\lambda_b],\theta_i,h] = \frac{\int_{\lambda_a}^{\lambda_b} \rho_{\lambda,\varphi}(\lambda,\theta_i,h)\cdot G_b(\lambda)d\lambda}{\int_{\lambda_a}^{\lambda_b} G_b(\lambda)d\lambda} \quad (3\text{-}10)$$

being $[\lambda_a,\lambda_b]$ the wavelength range and θ_i the incidence angle. The spectral or monochromatic hemispherical reflectance is defined as $\rho_{\lambda,h}(\lambda,\theta_i,h)$, being λ the first subscript, in this case, to indicate that the measurement is done just at a certain wavelength. The direct measurement of the hemispherical reflectance is most commonly carried out by devices like the integrating spheres, attached to a spectrophotometer. These devices will be explained in Chapter 6.3.

3.3.2 Specular reflectance

The standard definition for the specular reflectance according to UNE 206009:2013 [31] is "the ratio of the energy flux reflected by a surface in the specular direction to the radiation incident on it. The specular direction

is the one forming an angle with the normal to the surface equal to the angle of incidence of the incident radiation. The specular direction is on the same plane as the incident radiation and the normal to the surface and opposite to the direction of incidence. A certain angle of acceptance of specular reflectance, φ must be defined."

The solar near-specular reflectance is represented as $\rho_{s,\varphi}([\lambda_a,\lambda_b],\theta_i,\varphi)$, being $[\lambda_a,\lambda_b]$ the wavelength range, θ_i the incidence angle, φ the acceptance angle. As in the previous section, the first subscript is used to indicate that the reflectance is measured in the whole solar spectrum, while the second subscript is reserve to indicate that in this case, the reflectance is specular, measured with a certain φ. The solar-weighted specular reflectance is described in equation (3-11):

$$\rho_{s,\varphi}([\lambda_a,\lambda_b],\theta_i,\varphi] = \frac{\int_{\lambda_a}^{\lambda_b} \rho_{\lambda,\varphi}(\lambda,\theta_i,\varphi)\cdot G_b(\lambda)d\lambda}{\int_{\lambda_a}^{\lambda_b} G_b(\lambda)d\lambda} \tag{3-11}$$

In the case of concentrating applications, it is necessary to set an angle of acceptance (see 3.3.2.2), so, the reflectance of a mirror is defined as the ratio of incident power reflected by a mirror into the acceptance half-angle of the receiver φ. That reflected flux is denominated in that case specular reflectance (see Figure 3-8). Strictly speaking, the ideal specular reflectance is related to $\varphi = 0$, whereas the measurement at any small offset φ is more appropriately termed near-specular reflectance. Because of the angular radius of the sun, any element of an ideal mirror surface in a concentrator system will effectively reflect a cone of radiation with the same angular spread. Therefore, for an ideal reflector, the specular reflectance should be measured with a $\varphi \geq 4.70$ mrad.

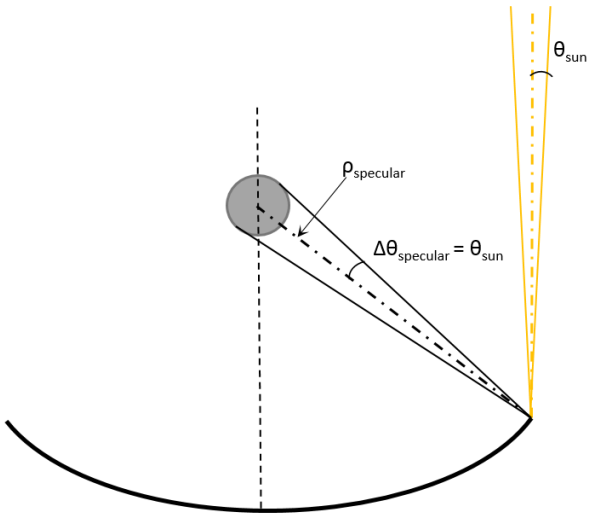

Figure 3-8 Rays reflected by a mirror in a PTC form a cone with a designated half-angle depending on the established specular limit

A real reflector will reflect a cone of solar radiation with an angular spread larger than the sun's due to imperfections like concentrator waviness, surface roughness, collector tracking tolerances, etc. (see Figure 3-9). The source of optical errors will be explained in detail in chapter 5.2.

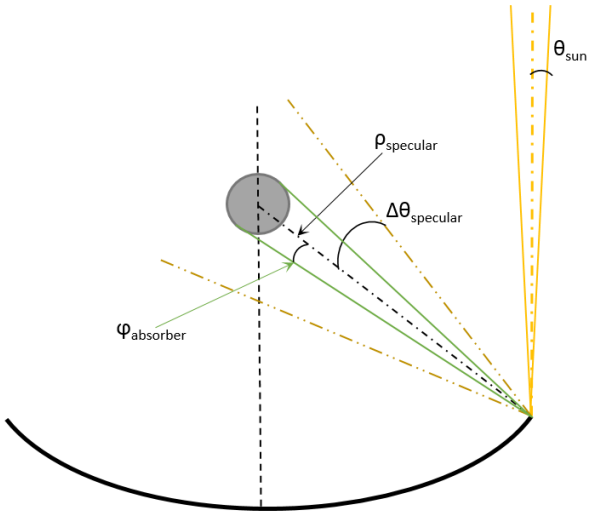

Figure 3-9 Rays reflected in a real mirror in a PTC

Therefore, all the solar radiation out of this established half-angle cone is denominated diffuse or scattered reflectance. Each solar receiver has a defined acceptance half-angle cone; Thus, each reflector can have different values of specular or diffuse reflectance depending on the absorber selected, since the acceptance angle will be different for each setup, for that purpose, the use of the term specularity gives more accurate information about the characterisation of a specular condition on a mirror, refer to 3.3.2.1.

The reflected power of a surface, more precisely the specular reflectance, is strongly related to the wavelength of the incoming wavelength solar radiation [33], as can be seen in Figure 3-10, mainly because the solar irradiance distribution is wavelength dependant.

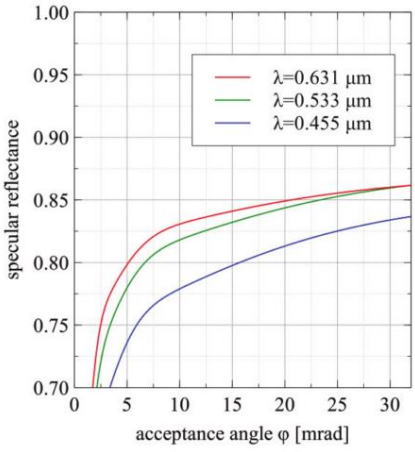

Figure 3-10 Specular reflectance for continuously varying acceptance angles for an aluminium reflector sample, measured at 3 wavelengths, angle of incidence 8° (A. Heimsath et al., 2015)

Due to that, loss of specular reflectance in wavelengths where the irradiance is high (Visible: $\lambda \approx 400 - 700$ nm) must be avoided. The specular reflectance is usually measured at an acceptance half-angle of $\varphi \leq 20$ mrad for CSP applications, so all the radiation within this half-angle cone can be considered near-specular [14]. Although for very specular materials, the difference between hemispherical and specular reflectance is small [34].

3.3.2.1 Specularity (near-specular reflectance)

For a solar mirror, it is not only important to reflect all the amount of incoming radiation possible but also to do so in a designated direction. The parameter known as specularity characterizes the capacity of a mirror to focus all the reflected light into the solar collector, or in other words, the specularity defines what percentage of the incoming radiation is reflected into the specular direction within the defined half-angle cone, φ. As stated before, usually for CSP applications the half-angle cone is $\varphi \leq 20$ mrad. Therefore, the specular reflectance is strictly defined as the reflected radiation with a $\varphi = 0$ mrad.

Specularity can be defined as in equations (3-12) and (3-13):

1. As solar specularity

$$specularity(s,\varphi) = \frac{\rho_{s,\varphi}([\lambda_a,\lambda_b],\theta_i,\varphi)}{\rho_{s,h}([\lambda_a,\lambda_b],\theta_i,h)} \tag{3-12}$$

2. As a spectral response specularity

$$specularity(\lambda,\varphi) = \frac{\rho_{\lambda,\varphi}(\lambda,\theta_i,\varphi)}{\rho_{\lambda,h}(\lambda,\theta_i,h)} \tag{3-13}$$

Since no mirror has an ideal specular behaviour, meaning, scattering of the outcoming radiation is usually expected, specular reflectance is always mentioned at a half-angle cone.

Depending on the angle of acceptance φ, the specularity could be different, so to compare values of different mirrors, the same measuring parameters and conditions must be compared in general terms.

The specularity is an important parameter to be characterised in a mirror since gives important information about the optical quality of a reflector or its condition. In a raw state, cleaned and out-of-the-production-line, the specularity gives information about the optical performance of a mirror configuration. Calculated in the solar field, gives information about the condition of the surface and its aging status.

Specularity can also be defined as the Root Mean Square (RMS) value of the beam widening, in milliradians, instead of percentage points [35] [36]. A perfect mirror would have a RMS value of 0 milliradians (excluding the solar broadening). The better the specularity, the smaller will be the RMS value of the beam spread from the reflective surface. If the specularity is described as RMS mrads, is giving information about the overall optical loss of specular reflection due to the mirror, in other words, the sum of all errors from the mirror which diminish the specular reflection. Specularity does not give any specific information about the soiling or aging of the mirror if not comparable with other data collected when the mirror is in a cleaned state.

Specularity is strongly influenced by the roughness of the substrate and the dust buildup over the first surface. Carlos Alcañiz *et al.* and the Photonics Technology Group (PTG) at the University of Zaragoza [37] did an experimental study to demonstrate the influence of the roughness of the substrate on the mirror specularity. They used Front Surface Mirrors (FSM) made by stainless steel AISI 304 coated with a silver layer through a Physical Vapour Deposition (PVD) process. The results of the hemispherical and the specular reflectance measure in the PTG laboratory are presented in Table 3-2:

Table 3-2 Influence of the roughness of the substrate in the solar hemispherical and solar spectral reflectance (C. Alcañiz et al., 2013)

Arithmetical mean roughness (Ra) (μm)	$\rho_{s,h}$ ([300-2500], θ_i, h)	$\rho_{s,\varphi}$ ([300-2500], θ_i, 30º)
0.00319	96.9%	96.9%
0.00623	96.6%	94.6%
0.03000	96.5%	91.6%
0.08520	93.9%	57.6%
0.10200	93.8%	44.7%
0.59800	89.5%	16.2%
0.71600	89.1%	4.5%
1.34000	89.0%	1.4%

The loss of intrinsic specularity in the mirror is originated by the roughness of the reflective surface or by the substrate where the reflector is deposited. In the case of study, the bigger the roughness of the steel substrate the bigger the scattering produced by the mirror, so a less specular light is reflected. Then, the roughness of a substrate is a key parameter to manufacture high-quality mirrors for concentrated solar plants. A simple sketch of how the roughness affects the specular beam profile can be seen in Figure 3-11. The scattering theory will be explained in chapter 3.3.3.

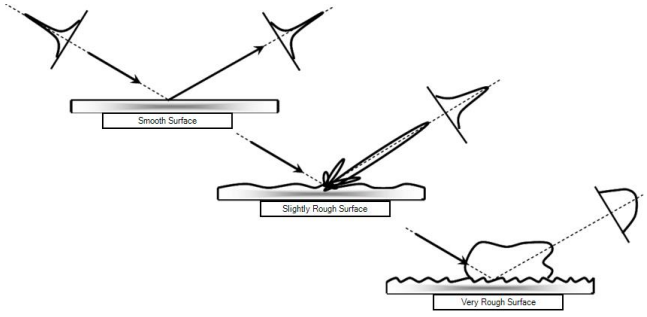

Figure 3-11 Transition from specular reflection to diffuse scattering due to the roughness of the surface (Peverini, 2005)

3.3.2.2 Acceptance angle of a receiver ($\varphi_{receiver}$)

A reflector is a shaped surface which collects parallel light beams and redirects them to a defined focus or objective, in the case of solar reflectors, it concentrates the light in a receiver[4]. All the receivers used in CSP have a related angle of acceptance of specular reflectance ($\varphi_{receiver}$). As stated in the UNE 206009:2013 [31], is the "angle defined by the specular direction and the direction of the admissible maximum dispersion of reflection on the surface".

The acceptance angle φ is a characteristic of the solar energy collector system and thus it should be considered to obtain the most accurate reflectance measurement. In a concentrating collector the acceptance angle can be calculated as in equation (3-14) [38]:

$$\varphi_{absorber,geometrical} = \arctan\left(\frac{diameter_{receiver}}{distance_{mirror-receiver}}\right) \tag{3-14}$$

For a PTC, like the Eurotrough-150, where the outer diameter of the receiver is 0.07 m and the distance mirror-receiver is about 2.88 m, results in a $\varphi_{\text{receiver-PTC}} \approx 24$ mrads. Most commercial PTC designs have acceptance angles within the range 17 - 34 mrads. For the tower systems, since the distance mirror-receiver is not constant, the acceptance angle in a tower system can not be considered constant for all the heliostats in the collector field area as can be depicted from the Figure 3-12.

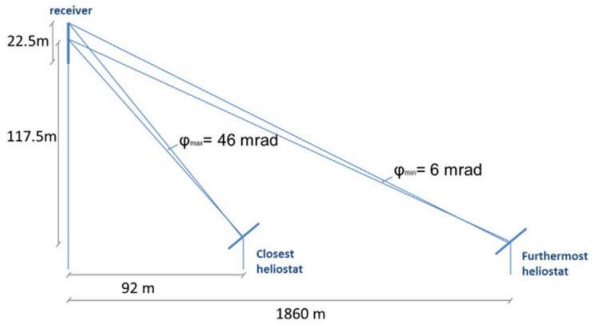

Figure 3-12 Acceptance angle of the receiver in the solar tower system CESA-1 located at the Plataforma Solar de Almería in Tabernas, Spain (Sutter, 2017)

The design of a tower heliostat field is aimed to maximise the solar irradiance collected by the field, depending on the position of the sun during the day and its change over the year. For designing and optimization of the solar field, refer to [5]. A summary of recent studies about software and modelling programs used in a PTC system can be found in [39].

If the specular reflected beam of the mirror ($\Delta\theta_{specular}$ or angular spread φ in Figure 3-9) has a large half-cone

[4] In a PTC system, absorber is the steel tube and receiver is the sum of the receiver tube and the glass envelope tube. In a tower system, it is usually called just receiver, it means that there is no substantial difference between a receiver and a absorber in a tower system.

angle in comparison with the receiver acceptance angle, $\varphi_{receiver}$, the efficiency of the absorber will not be optimised. There is the rule of choosing $\varphi_{receiver}$ equal to twice the RMS width θ of the radiation distribution incident on the receiver or $\sigma_{collector\ system}$, if the reflected beam is characterised as a Normal distribution. This rule corresponds to intercepting 95% of a Gaussian distribution [23]. As can be seen in Figure 3-13, for φ larger than 25 mrads, the specular reflectance of a mirror can be considered constant except for the Alumium mirrors. Designing collectors with broader acceptance angles is difficult since either the diameter of the receiver is larger or the distance receiver-mirror is shorter, so maximising the specularity of a mirror is important for the operation of such solar power plants. For instance, recommended acceptance angles for commercial PTCs collectors are in the range 8.7 - 17.5 mrads with geometric concentration ratios from 20 to 30 [40].

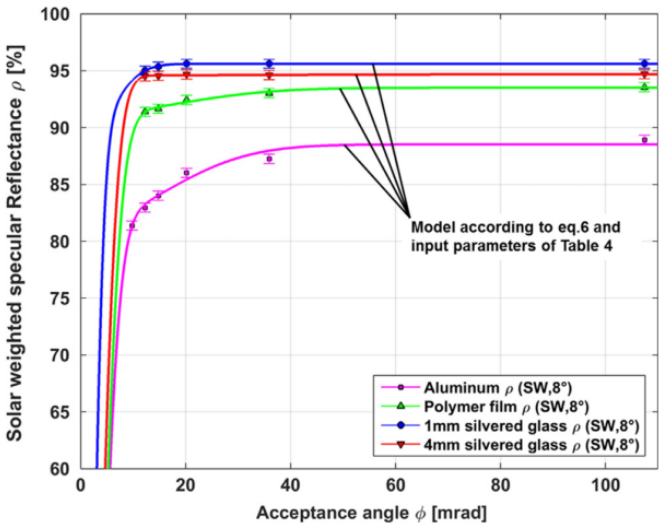

Figure 3-13 Specular reflectance $\rho_{s,\varphi}$ ([250-2500], 8º, φ) versus acceptance angle for four solar mirror materials (Sutter, 2016)

The quality of specularity in a mirror can be assessed by the measurement of the specular reflectance at various acceptance angles and various wavelengths and compare the results with the measured hemispherical reflectance [41].

3.3.3 Diffuse reflectance

In general terms, according to UNE-EN ISO 9488:2001 [32], the diffuse radiation is the solar hemispherical radiation minus the direct[5] solar radiation. In the case of a reflection, the diffuse reflectance is all sun radiation reflected from the mirror outside the half-angle cone defined as specular (that is, the acceptance angle, φ). The reduction of the specular reflectance in a reflector is caused by two mechanisms:

1) by absorption of the incident light
2) by the scattering of the reflected solar beams in all direction but the defined as the specular one

Being the scattering the main loss factor of specularity in a mirror [13]. If a parallel light beam of a certain λ_{light} impinges a surface with microscopic irregularities of a size equal or greater than the λ_{light}, the incident beam will

[5] Direct solar radiation is an outdated concept, it is usually used near-specular or specular depending on the context.

face a different slope than the slope normal to the mirror, so it will be reflected according to the first law of reflection with other direction than the incidence angle of the light beam to the mirror [12] [13]. Each light beam might face a different surface slope, causing a multidirectional reflection pattern, or scattering distribution, as can be seen in Figure 3-14.

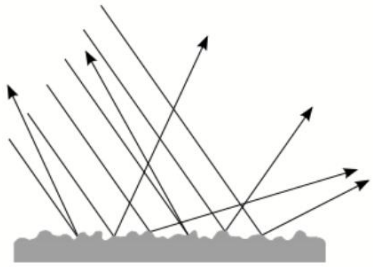

Figure 3-14 Diffuse reflection beams caused by surface irregularities

Scattering is caused mainly by two phenomena: surface roughness, as seen in Figure 3-14, and dust or soiling over the surface of the mirror. The scattering produced by soiling is very difficult to model, as its angular distribution depends heavily on the size and shape of the particles over the surface of the mirror [13]. A perfectly diffusing surface is defined as a surface whose reflected radiance is independent of the direction of viewing and hence obeys Lambert's law.

As seen in Figure 3-14, surface irregularities cause the reflection to be non-specular. The effect of surface roughness on the optical properties of materials was first studied by Lord Rayleigh. If the size of the irregularities is around the order of the wavelength or larger, the interaction can be described by geometrical optics. However, if the surface irregularities are much smaller than the wavelength, the optical behaviour can be explained by diffraction phenomena [42] [43]. The scattering on this case is called Rayleigh scattering. Its scattering profile can be approximated as the profile of a Lambertian source of intensity. The Lambertian source is an ideal source in which the spectral intensity (power per unit wavelength per unit solid angle per unit area normal to the direction of reflection) of the emitted light is independent of both incidence direction and reflectance direction. The emitted intensity obeys the Lambertian cosine law, which states that the radiance of a Lambertian surface, *I(θ)*, (geometric distribution of the radiant exitance M of a source) is proportional to the cosine of the angle between the surface normal and the direction of the incident light, θ, then $I(\theta) = I_0 \cos\theta$. This assumption is quite accurate as measured by Ignacio Salinas *et al.* in [44], see Figure 3-15.

The scattering function profile can be approximated on a mirror by the mirror surface Arithmetical Mean Roughness (Ra) or, in the case of a solar field mirror (soiling over the mirror surface), by the size of particles deposited in it. The intensity ratio of the scattered light incident, $\frac{\bar{I}_s}{I_0}$, onto a particle surface is given by equation (3-15):

$$\frac{\bar{I}_s}{I_0} = \frac{1}{r^2}\left(\frac{2\pi}{\lambda}\right)^4 \alpha^2 \sin\theta \tag{3-15}$$

where $\bar{I}_s$ is the scattered radiation intensity flux per unit time (seconds), I_0 is the incident beam radiation intensity, r ($\phi_{particle}$ / 2) is the average particle radius, λ is the wavelength of the incident radiation, α is the proportionality factor (if a surface is isotropic, the α is by definition identical for all angles of reflectance) and θ is the reflected light angle versus normal incidence [45].

In the same case as for the surface R_a, if the characteristic size of the particle is smaller than the wavelength of the beam ($\phi_{particle} < \lambda_{light}$), the scattering produced from particles is also called Rayleigh scattering [45]. Otherwise, if the characteristic size of the particle is bigger than the wavelength of the beam ($\phi_{particle} > \lambda_{light}$), the scattering profile will be more directional and is known as Mie scattering.

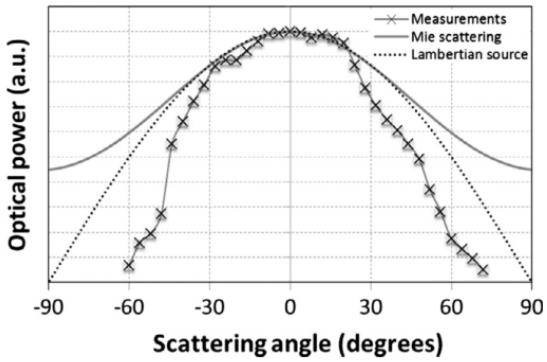

Figure 3-15 Scattering pattern for particles with a $\phi_{particle} \approx$ 100nm measured at a wavelength of 650nm. Comparison with a Lambertian source of the same wavelength (I. Salinas et al., 2016)

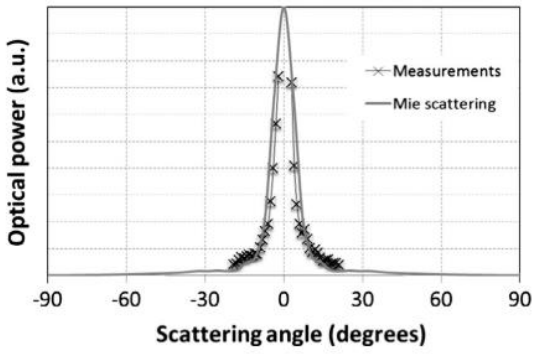

Figure 3-16 Mie scattering pattern for particles with a $\phi_{particle} \approx$ 5000nm measured at a wavelength of 650nm compared to a measurement of a dirt sample at the same wavelength (I. Salinas et al., 2016)

Salinas et. al. also offer a comparison of performance regarding diffuse reflection collected by each collector type, as can be seen in Table 3-3.

Table 3-3 Performance of the collectors regarding the collected diffused reflection (I. Salinas et. al., 2016)

Optical System	% of diffuse reflection collected	
	Lambertian Scattering	Mie Scattering
PTC	2.0	10
Central Receiver System	0.003 - 0.06	0.14 - 0.56
Dish	0.04	1.7

The relationship between the surface roughness and the scattered light is called Total Integrated Scattering (TIS), see equation (3-16), and was first described by [46].

$$TIS = \frac{\rho_{\lambda,d}(\lambda, \theta_i)}{\rho_{\lambda,h}(\lambda, \theta_i)} = 1 - exp\left(-\left(\frac{4\pi\delta_s \cos\theta_i}{\lambda}\right)^2\right) \quad (3\text{-}16)$$

Being the δ_s the roughness of the scattering surface. According to this expression, for smaller λ and lower θ_i, high scattering and vice versa.

4 MIRRORS

A concentrator is a mirror (or reflector, in this thesis it will be considered both definitions as synonyms) with the proper shape to focus the incoming solar radiation into a designed point or line.

Usually, a concentrator in a solar field has an aperture area between 70 m^2 (Acurex PTC) for a PTC till areas larger than 864 m^2 like the SenerTrough collector used in Noor 1 Plant. In the case of solar tower plants, there are heliostats from 7.22 m^2 like the ones used by the Commonwealth Scientific and Industrial Research Organisation (CSIRO) till aperture areas to 138.7 m^2 like the ones installed in Sevilla by Abengoa (ASUP 140) or to 178 m^2 like the ones developed by Sener [47].

To achieve such a large area, they are assembled by several reflectance surfaces called "facets". These facets could have a parabolic shape in the case they will be used in a PTC or could be quasi-planar (see Figure 4-1), like the ones used in a heliostat for a solar tower power plant.

Figure 4-1 Crescent Dunes (Tonopah) Heliostat. 6x6 ft each facet, 35 facets each heliostat, total surface area of 116 m^2

The reflector is the first principal component of a STE plant. The overall cost of a solar field in a STE plant is around 36% - 50% of the total CAPEX depending on whether it is a ST or a PTC technology plant. And within the cost of the solar field, mirrors can account for between the 21% till 40% of the CAPEX [48] [47].

The need of fewer heliostats/collectors per MW installed in a power plant could be a way of reducing the LCOE, but the use of non-completely specular mirrors leads to increase the number of heliostats/collectors needed to fulfil the solar flux requirements in the receiver. In the case of a ST of 50 MW, this could mean an increase of heliostats needed from 3.2% to 9.6%. In the case of a PTC, the range extends from 3.4% to 10.4% depending on the type of mirror configuration used [37].

Mirrors for STE plants can be classified by the following approaches: depending on geometrical considerations or the setup used in its manufacture, see Figure 4-2.

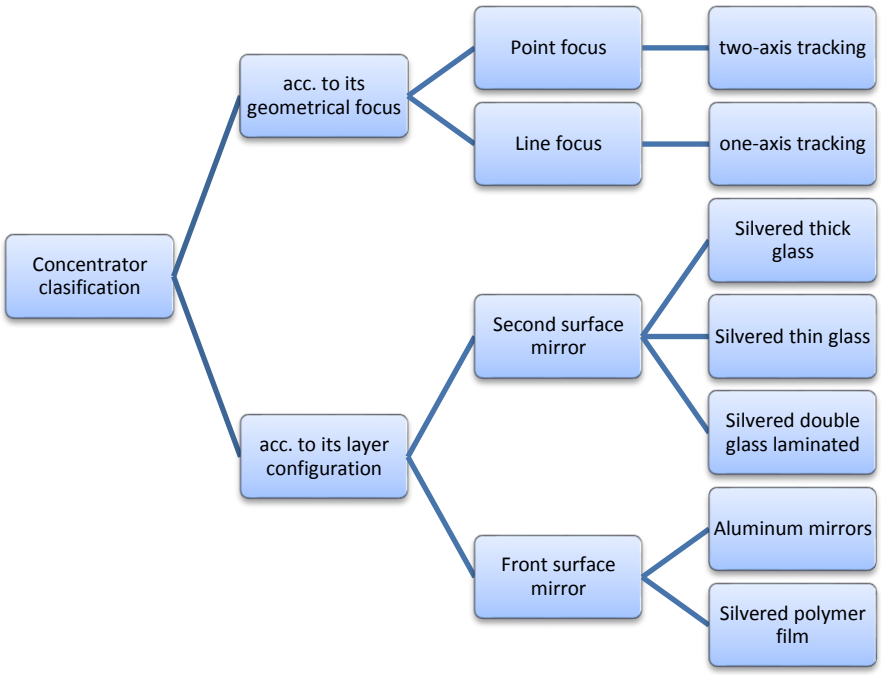

Figure 4-2 Concentrator classification categories

Any layer configuration can be used as a point focus concentrator or as a line focus concentrator. Concentrators can be also classified as imaging or non-imaging concentrators and as continuous or segmented surface concentrators. Regarding the geometrically focus configuration, the concentrator can focus the solar radiation in two different patterns, based on the shape of the reflector: over a single point or a line, see Figure 4-3. Using one or another shape depends on the collector used, i.e., PTC and LFR are line-focusing concentrators, but heliostats or parabolic dishes are point-focusing concentrators.

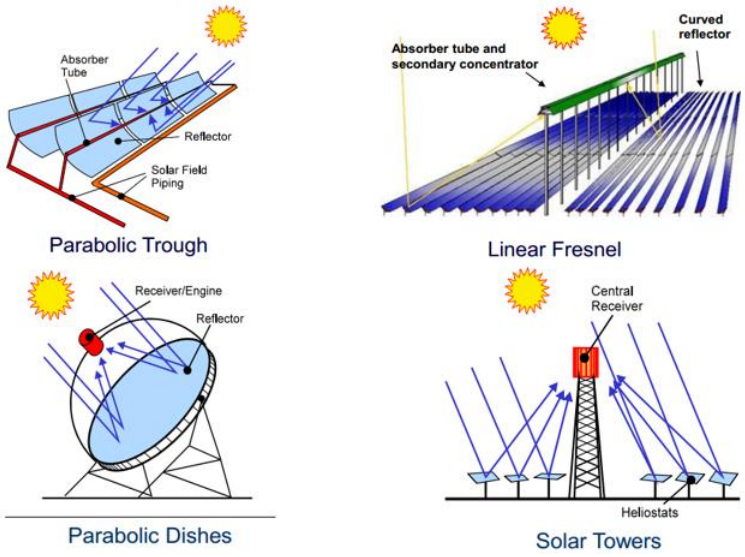

Figure 4-3 Types of concentrators according to its geometrical focus. Line focus: PTC and LFR. Point focus: parabolic dishes and ST

The manufactured shape quality of the concentrator plays a key role in its optical efficiency. Irregularities in the shape quality are defined as slope deviations. The variations over the nominal shape can influence the reflected beam and provoke a deviation of the reflected ray by twice the slope deviation angle of the respective mirror surface (see chapter 5.2 for more information). Given the purpose of this work, it is decided to outline only the classification according to its layer configuration.

There are a lot of materials which combines a series of properties making them an ideal candidate to be used in a mirror. For instance, the next Figure 4-4 shows a comparison of the reflectance spectrum of several reflective materials.

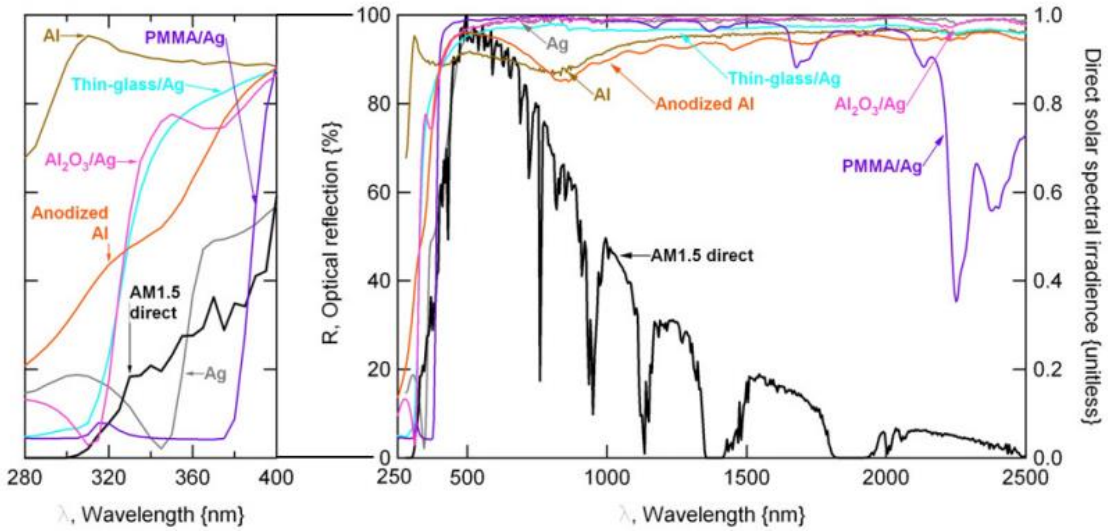

Figure 4-4 Hemispherical reflectance, incidence angle 8°, for candidate CPV optical component materials. The normalized direct solar spectral irradiance (AM1.5 in ASTM G173) is provided for reference (Miller, 2009)

But for better performance in STE plants, reflective materials must be attached to other layer systems to form a proper solar reflector and to protect the reflective layer from the environment to avoid fast aging. In the next subsections, the most proven mirror configurations will be described to give an overview of what to expect in the solar field when measuring reflectance on site. Next, a detailed description will be presented to review the main materials and configurations suitable for concentrating solar thermal technologies [49].

4.1 Second surface mirrors

The second surface mirror (SSM) configuration is named so because the reflective layer (usually of a silvered-base material) is deposited on the back of a transparent layer or added onto a back structure. This transparent layer is also the substrate which protects the reflective layer. These types of mirrors are also known as silvered-glass mirrors because the substrate is normally a glass layer. Silvered-glass mirrors are the most employed in STE plants given its demonstrated stability over the life cycle of a plant and almost neglectable loss of optical properties. Depending on the thickness of the glass and the layer setup, it can be categorized into three types.

4.1.1 Silvered thick glass mirrors

A thick glass layer could be defined as a layer with a thickness range between 3-5 mm, being 4 mm the standard commercial thickness. Monolithic glass mirrors or floated glass mirrors are also definitions for such configuration.

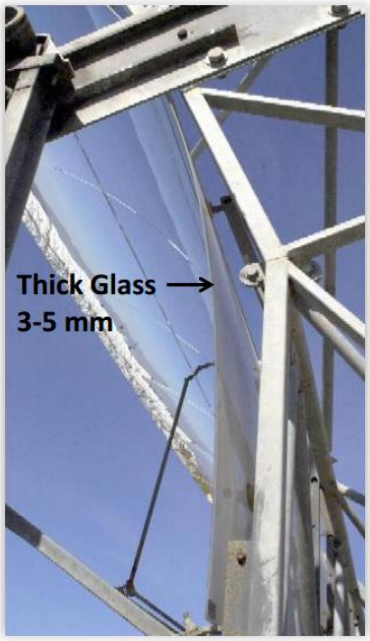

Figure 4-5 Thick glass mirror installed in a Eurotrough Parabolic Trough Collector.

An advantage of thicker glass mirrors (> 3 mm) over thinner mirrors is that their mechanical strength enables them to withstand wind loads without requiring special backing structures to avoid breakage and maintain their shape. Usually, they are fixed to the collector through bonding clamps (typically named pads), as it can be seen in Figure 4-5.

The glass layer in this setup is used as a top protective layer, therefore it must be very transparent to solar radiation. That is the reason why the glass used in STE plants is called "water-white" or "extra-clear" glass. The water-white is a silica-based glass with less than a 0.02 % w/w of ferric oxide (typically 0.01 % w/w) [26]. Is well known that ferric oxide absorbs light radiation in the infrared spectrum (around 1000 nm – 1100 nm), as can be seen in Figure 4-6.

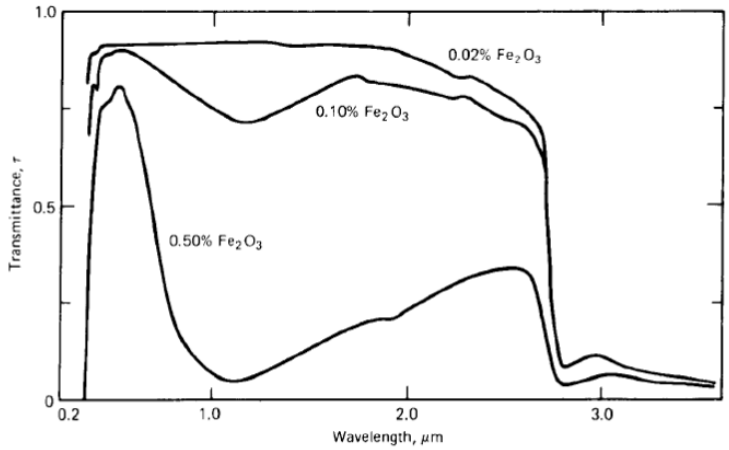

Figure 4-6 Spectral transmittance of 6-mm-thick-glass with various iron oxide contents. A high concentration of Fe^{2+} in the glass leads to the appearance of an absorption band in the glass centred at approximately 1100nm (Dietz, 1954)

In this type of mirror, it has been noticed that the loss of specular reflectance overtime was not increasing as rapidly as expected. On the contrary, the specular reflectance was increasing and not due to the aging of the reflective layer but because of the change in the transmittance and absorption spectrum of the glass layer. This phenomenon is called "glass solarisation" [50] [13]. As can be seen in Figure 4-7 and Figure 4-8, both hemispheric and specular reflectance in the range of 900 nm to 1200 nm increase over time.

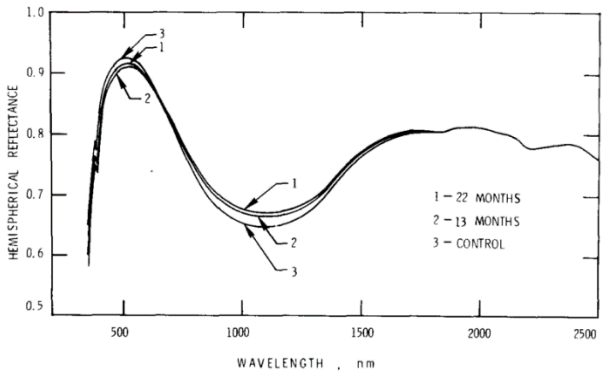

Figure 4-7 Hemispherical reflectance of two aged silvered glass mirrors and a control sample (Pettit and Freese, 1980)

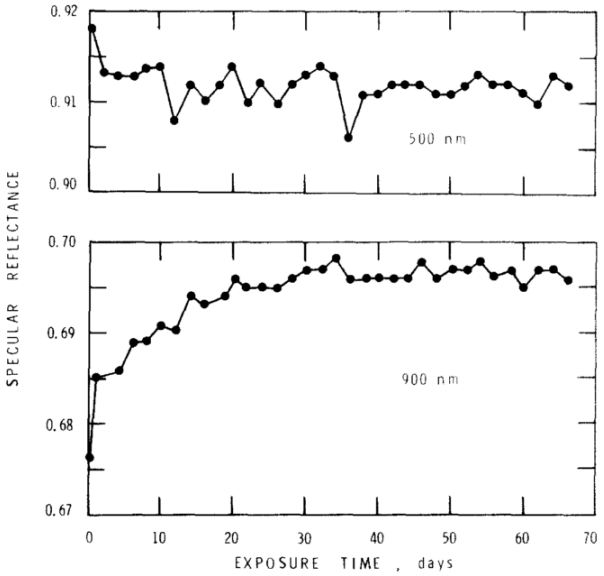

Figure 4-8 Specular reflectance at wavelengths of 500 nm and 900 nm for a silvered glass mirror cleaned every two days over 66 days of outdoor exposure (Pettit and Freese, 1980)

It seems to be that the long-term exposure reduces the Fe^{2+} to Fe^{3+}, which has no absorption band at 1100 nm (see Figure 4-9). There are some studies about the root cause of the solarization [51], which at the beginning of the mirror life cycle, this phenomenon increases lightly the reflectance of the glass (A standard low-iron-glass has a luminous transmittance around 91-92 %), since due to the UV exposure, Fe^{2+} is reduced to Fe^{3+}.

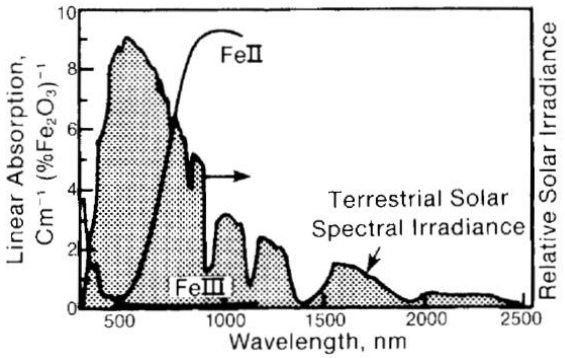

Figure 4-9 Absorption coefficients of Fe^{2+} and Fe^{3+} in Soda-Lime Glass (Coyle, 1981)

Silver is typically used as a reflective layer. Silver has a hemispherical reflectivity of 97% and is known to be one of the best solar reflectors. However, it may corrode under atmospheric conditions, consequently, it must be protected [52]. The first mirror generation used a back protective layer system comprised of two materials. First, a copper layer over the silver is applied to slow down the silver corrosion (copper acts as a sacrificial anode as it has a lower standard electrode potential) and to prevent transmitted UV-light through the silver layer to damage back protecting coats. Over the copper, lead-based protective paint is applied to prevent diffusion to the silver layer and protection against the UV radiation. A first-generation mirror could be portrayed as depicted in Figure 4-10:

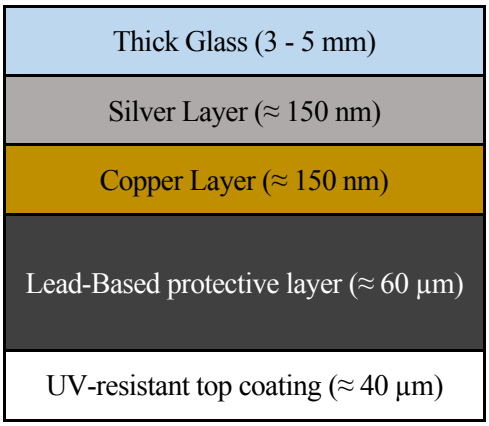

Figure 4-10 Monolithic silvered glass mirror layer setup

State-of-the-art 4 mm silvered-glass mirror reflectance achieves solar-weighted hemispherical reflectance values around 94.7 %. Although this kind of material and layer configuration has given a proven performance in a solar field for many years, for SSMs, the copper layer might be replaced by a 100 Å SnO_2 to cut production costs and comply with environmental regulations. Also, because of the environmental and health issues, lead content in the protective layer has been reduced from 20 % w/w to less than 1 % w/w[6], or, in the best cases, the lead-based paints have been replaced by lead-free paints or antioxidant pigments with similar proven durability results [53].

4.1.2 Silvered thin glass mirrors

This kind of mirror setup uses the same layer configuration as the above described, but instead using a thick glass layer of around 3 mm - 5 mm, a thin layer of glass around 1 mm performs as the main substrate.

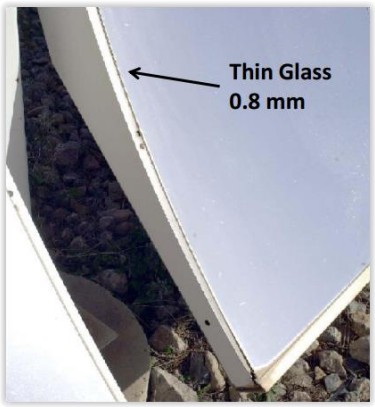

Figure 4-11 Thin glass mirror installed in a parabolic trough collector, Acurex 3001

Light passing through an absorbing material is attenuated as a function of the absorption coefficient and the thickness of the material [45]. Since the glass substrate is 80 % thinner than the thicker ones, it absorbs less light and the radiation transmission to the reflective layer is higher. Therefore, the reflectance of this kind of setup is higher. The layer configuration is the same as for the thick glass (see Figure 4-10).

[6] In the US, since 2009, the lead allowable in most paints is now 0.009% w/w (90 ppm) [https://www.atsdr.cdc.gov/csem/csem.asp?csem=34&po=8] while in the EU, the REACH regulation stablishes a limit in less than 0.1 % w/w (1000 ppm) weight by weight. [https://europa.eu/capacity4dev/unep/documents/global-report-status-legal-limits-lead-paint].

The main disadvantage of using thinner glass is that the mechanical strength is not high enough to be a self-supporting structure and it makes necessary to glue them to metal or composite structures as a substrate (see Figure 4-11), making it more expensive. Besides, this configuration usually supports fewer wind loads than the thicker glass ones, depending on the substrate.

Both thicker and thinner glass reflectors have passed several years of Accelerated Exposure Testings (AET) and Outdoor Exposure Testings (OET). Less than 4 percentage point loss of hemispherical reflectance was reported for both setups [54]. In the case of thick glass reflectors, the OPAC group did a study exposing several samples of thick glass mirrors to AETs and OETs. For an AET, the highest decrease in solar-weighted hemispherical reflectance reached 3.3 percentage points. For the case of the OET, the maximum change in reflectance was 4.3 percentage points [55]. Also, the choice of the adhesive between the steel substrate and the mirror has been observed to affect the performance of them in outside exposure and corrosion phenomena have been detected [53]. For comparison, the next figure includes a reflectance spectrum of a 1 mm glass mirror sample and one with 4 mm.

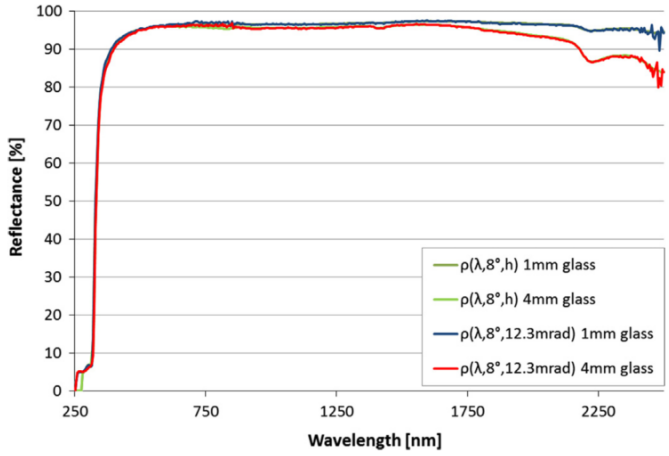

Figure 4-12 Comparison of hemispherical and specular (φ = 12.3 mrad) reflectance spectrum of a 1 mm and 4 mm silvered glass reflector (Sutter et al., 2016)

4.1.3 Silvered double glass laminated

The double glass laminated mirror just uses as back protective coating another layer of shaped glass, serving as an anticorrosion layer. This kind of setup has been used in the automotive industry for a while, so its production quality is well established, but installing in a solar field is still ongoing since the costs are much higher than the other alternatives. A pilot plant installed in the Plataforma Solar de Almería (PSA) uses this kind of mirror configuration for testing purposes[7] but even the original equipment manufacturer, Guardian, does not sell this type of mirrors anymore.

[7] https://sfera3.sollab.eu/access/#infrastructures

4.2 First surface mirrors

The first surface mirror (FSM) configuration is named so because the substrate is an opaque material, like polished aluminium or a polymeric substrate, and the reflective surface is placed upon it. Besides, the top protective layer covering the reflective surface usually has a thickness of around 3 - 5 μm. So, the FSM are usually thinner than the SSM. There are two available types of FSM, aluminium mirrors, and silvered polymer mirrors.

4.2.1 Aluminium mirrors

The most extended aluminium reflectors are composed of a polished aluminium sheet as the substrate, an enhanced aluminium as the reflective material and a top nano-composite protective coating like the one used by Alanod GmbH [56]. A typical aluminium mirror configuration could be pictured as follows:

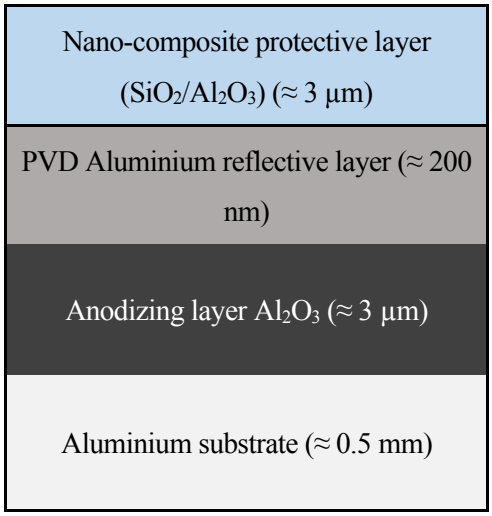

Figure 4-13 Aluminium mirror setup

Aluminium has a hemispherical reflectance $\rho_{\lambda,h}$ of around 88% - 91% in the range 250 - 2500 nm [57]. Aluminium reflectors are too thin and need a support structure that might increase the cost of the concentrator. Besides, its manufacturing process creates a non-smooth surface that leads to high scattering of the reflected rays and the specular reflectance shows a significant decrease when the acceptance angle is reduced, as can be seen in Figure 4-15. That great decreasing in the specular reflectance makes this kind of mirrors only suitable for low-temperature concentrating applications [53] [58].

The loss of specularity in the FSM could be explained by the spectral characterization comparison between a monolithic glass mirror (named as "floated glass mirror") and an aluminium mirror (named "commercial product 1") in the next Figure 4-14 [37].

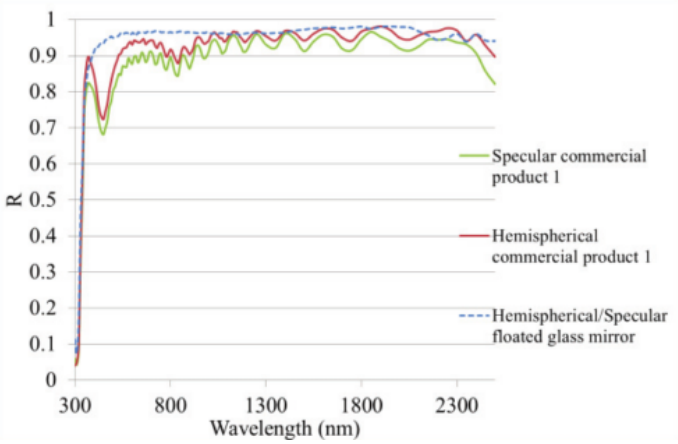

Figure 4-14 Front Surface Mirror vs Reference (Alcañiz et al., 2015)

In the figure above, the loss of reflectance in the visible range is caused by the protective layers above the silver coating. All silicon oxides exhibit stronger absorption bands below 300 nm. Also, if Aluminium is used as a reflective material, the reflectance will be lower due to the absorption band of the Aluminium in the visible range (interband transition of aluminium at 860 nm). As can be seen in Figure 4-15, the Aluminium reflectors present a high scattering profile according to its specular reflectance spectra. The lower the acceptance angle, the higher the specular reflectance. The scattering losses peak in the $\lambda \approx 400$ nm is approximately 15 percentage points. The valleys (up and downs) in the spectra are originated by interference effects. These interference patterns are produced by the inhomogeneities of thickness and quality in the dielectric and protective layers, diminishing the total solar reflectance [59].

For this reason, its high scattering added to its low hemispherical reflectance make them not adequate for solar applications with high concentration ratio.

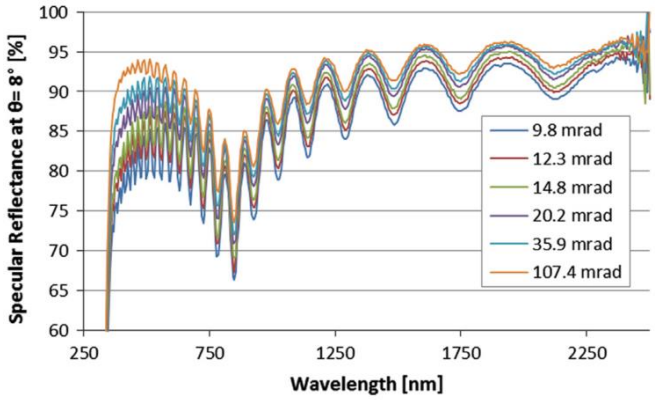

Figure 4-15 Specular reflectance spectra of an enhanced aluminium mirror plotted for different acceptance angles at $\theta_i = 8°$ incidence angle (Sutter et al., 2016)

The optical durability in the solar field has been proved to be poorly, losing specular reflectance after AET [58]. For instance, after a damp-heat cycling test, Uppsala University measured a decrease in the solar-weighted specular reflectance around 72 percentage points (From 79 % to 7%) over a polymer-protected evaporated

aluminium reflector [60]. Nevertheless, a top coating such as a SiO_2 sol-gel deposited layer has shown improved results after a 5 years' OET at the Tabernas Desert (PSA). The maximum lost in monochromatic specular reflectance was 3.7 percentage points [61]. A summary of accelerated tests done in this kind of reflectors can be found in [55].

Another study done by Sutter *et al.* [62] with a typical aluminium reflector configuration revealed the specular reflectance losses after 10 years of outdoor exposure. The specular losses caused by corrosion phenomena are expected to be in the range of 0.5 - 3.0 ± 1.4 percentage points depending on the outdoor exposure site. In the same exposure period, specular reflectance losses caused by scattering are expected to be in the range of 6.6 ± 1.4 percentage points. The reflectance losses caused by scattering are almost independent of the exposure site, consequently, they are inherent to the aluminium setup itself.

Besides, although manufacturers like Alanod GbmH have carried out AETs on its products for solar applications, they still must improve its durability but are suitable for some applications (intermediate-temperatures) and several facilities of "small-sized" collectors.

4.2.2 Silvered polymer film mirrors

This configuration uses a polymer film as a substrate and as a top protective coating. Silver is used as a reflective material.

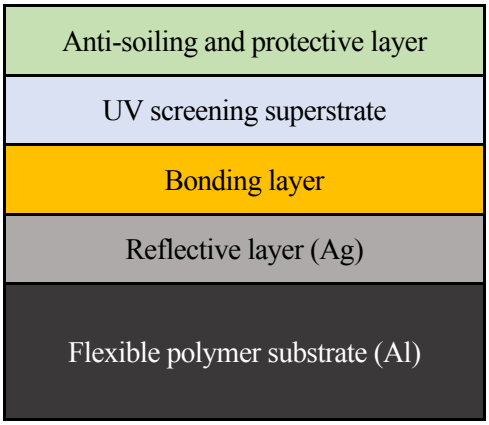

Figure 4-16 Standard silvered polymer mirror configuration

These mirrors are more flexible than other commercially available and have the potential to adapt to any desired shape. Albeit due to the temperature limits of the polymer film, this setup cannot withstand temperatures greater than 80 ^{0}C, which limits its use in some operations.

Manufacturers like Skyfuel Inc.[8] claims that the specular reflectance of this setup (ReflecTech® PLUS) reaches values over 91% at 7.5 mrads and has been tested outdoors for several years in the Solar Electric Generating Station (SEGS) without any sign of degradation. One major disadvantage of the polymer reflectors is that they degraded rapidly after several brush washing cycles. Samson *et al.* published a study where highlights the effects of contact cleaning methods on this kind of setup. After 100 brush cycles (almost two years of simulated

[8] Skyfuel Inc. filed for bankruptcy in 2019.

operation), the specular loss was around 6 percentage points (λ = 660nm, θ_i = 15, φ = 12 mrad) [63]. Although the authors of this work stated that a proper cleaning method (with a soft brush) might avoid such type of degradation.

Related to the reflectance spectra, in the case of the polymeric-based mirror, as clearly seen in Figure 4-17, it absorbs light in the Ultraviolet range and the Near-Infrared Range, losing thus overall reflectance.

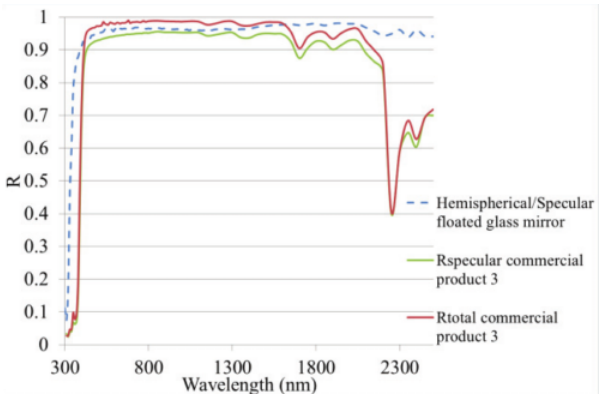

Figure 4-17 Polymeric-based mirror vs reference, (Alcañiz et al, 2015)

However, since the visible range of light contains more energy than the UV or NIR, the overall specularity of the polymer-based mirrors is better than in the Aluminium mirrors, not only due to that but to the better reflectivity properties of the Ag in comparison with Al. See Table 4-1 for a reflectance comparison between all configurations.

In addition, the vacuum process involved in their production and the roll-to-roll packaging still cause many surface defects that result in high directional scattering. There is still a lot of room for improvement in this kind of configuration to make it suitable for concentrated solar applications.

In the last years, innovative approaches have been developed using these configurations. A promising low-cost reflector material, developed by NREL under a subcontract with Science Applications International Corporation (SAIC), has a silvered specular substrate protected by an alumina coating, several microns thick. That configuration is still under development and has not reached the pilot phase yet [64].

4.3 Ideal properties in a mirror

A mirror must be designed to deal with the most extreme weather conditions which will suffer in the site location and to withstand the fatigue of the several cleaning cycles it will face in the lifetime of a STE plant. The main requirements of a proper solar reflector for power generation might be resumed as follows:

- High specular reflectance along the whole solar spectrum: > 94%
- Optical error ≤ 3 mrad [65]

- Expected lifetime over 30 years (proven against environmental factors. Proven stability relating the bonding with the collector structure)
- Stable optical efficiency and geometrical quality
- Antisoiling properties are a nice-to-have feature
- Support operational wind loads of 15 m/s and maximum wind loads of 33 m/s (i.e., SENERtrough = 33 m/s; Flagsol SKAL ET-150 = 31.5 m/s). Sunshot initiative roadmap > 38 m/s

To be able to be cost-competitive in terms of LCOE with other Fluctuating Renewable Energy Sources (FRES), an ideal advanced reflector must have the following properties too [66]:

- High abrasion resistance (reflectance loss < 1 %)
- Strong adhesion of the coating/layers
- High transmittance of the front-surface coating; RMS specularity below 1.6 mrad

Regarding its reflectance properties, the next table includes hemispherical and specular reflectance values of the above-described mirrors [34] [37] [49]. The hemispherical values are comparable each other but because of the wavelength-dependent scattering, in the case for the specular reflectance, only values obtained in the same conditions (λ range, same θ_i, same φ) are analogous. See Figure 4-18 for a comparison between Aluminium, Silvered glass, and polymer-based reflectance spectrum.

Table 4-1 Solar hemispherical and specular reflectance values of different mirror setups [37] [67]

Type of mirror configuration	Solar weighted hemispherical reflectance (acc. to ASTM G173-03:2020 [25])	Solar weighted specular reflectance
Silvered thin-glass	94.0 - 96.0 %	
Silvered thick-glass	94.0 - 95.0 %	95.1% (φ = 30 mrad)
Aluminium	85.0 - 94.0 %	88.0% (φ = 30 mrad)
Silvered polymer film	90.0 - 94.0 %	92.1% (φ = 30 mrad); 91.0% (φ = 7.5mrad) from Skyfuel

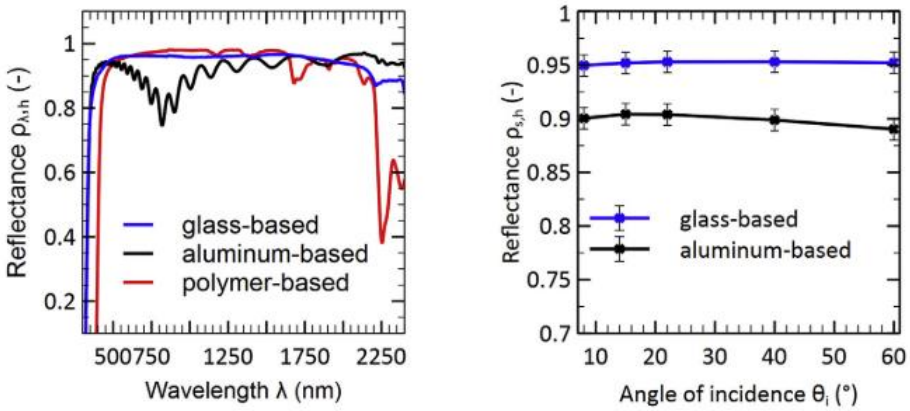

Figure 4-18 Left: Hemispherical reflectance measured at a near-normal angle of incidence for Aluminum, glass and polymer-based mirrors. Right: Measured solar weighted hemispherical reflectance for incidence angles between 8° and 60° (Heimsath, 2019)

According to AENOR UNE 206016:2018 [15], a mirror can be considered near-specular if it complies with the next two criteria, quoted:

1. The difference between the experimental values of near-specular reflectance, $\rho_{s,\varphi}(\lambda, \theta_i, \varphi, T_s)$, at a λ in the range λ = [400, 700] nm and $\theta_i \leq 15º$, measured for $\varphi \approx 7.5$ mrad and $\varphi \approx 23.0$ mrad must be less or equal than the experimental error (typically ± 0.003). The two measurements must be accomplished in the same conditions (particularly with the same instrument and in the same point of the mirror surface), except for the φ angle. This test must be repeated at least at three different points of the mirror surface.
2. The solar-weighted diffuse, $\rho_{s,d}$, reflectance at $\theta_i \leq 15º$ and 7.5 mrad < φ < 120 mrad, $\rho_{s,d}$ ($[\lambda_a, \lambda_b]$, $\theta_i \leq$ 15º, 7.5 mrad < φ < 120 mrad), measured with a high-quality spectrophotometer equipped with an integrating sphere with diameter not less than 150 mm and configured to leave the specular beam escaping with a light-trap accessory, must be less or equal than the experimental error (typically ± 0.003).

Not only are the original reflection properties in a mirror important, but its stability over time is a critical factor. To assess the durability of a reflective material or mirror layer composition, a series of aging test can be performed on it. As it has been mentioned before, there are two types of aging tests: outdoor exposure testing (OET) and accelerated exposure testing (AET). The purpose of these tests is to measure the loss of reflectance over time and to evaluate the degradation of the materials used. OETs are extremely dependant on the site location, which make the obtained results hard to extrapolate to other areas, so OETs alone are insufficient for an exhaustive durability study. Besides, an OET would have last decades to produce reliable results. For that reason, AETs can help to fill the data gaps and help to develop a good aging model of the mirror itself. There is still no international standard about how to carry out AETs in mirrors, but a list of standardised AETs collected by international institutions could be found in [55].

5 PERFORMANCE IN A SOLAR CONCENTRATOR

The efficiency of a solar concentrator is defined by the specular reflectance of the mirrors and by the optical accuracy of its shape. There are several sources of errors which lead to decrease the theoretical efficiency in a solar concentrator. From the reflectance material itself, the quality of the collector construction to errors coming from the direct operation as soiling or sun position tracking errors. The characterisation of all these failures will help to better assess in which of them the technicians should focus their efforts since not all of them cause a decrease in the efficiency in the same proportion. Furthermore, to produce accurate models of the solar reflectance in the solar field, the sources of errors in a solar collector must be studied. This chapter tries to collect a list of these errors and how they influence the optical performance on the field.

5.1 Estimation of the performance in a solar collector

The performance of a solar collector system represents the percentage of the beam solar irradiation reaching the concentrator aperture plane. In the case of a PTC, it can be summarised in equation (5-1):

$$\eta_{collector} = \eta_{optical} \cdot \eta_{thermal} = \frac{Q_{collector \rightarrow trasnfer\ fluid}}{Q_{sun \rightarrow collector}} \tag{5-1}$$

In other terms, it can be defined as the percentage of the solar irradiation (energy) reaching the collector which is transferred to the HTF. The net thermal energy absorber by the HTG can be defined as in equation (5-2):

$$\begin{aligned} Q_{net} = {} & (solar\ irradiance\ reaching\ the\ reflector) \\ & \cdot (\%\ of\ the\ irradiance\ intercepted\ by\ the\ absorber) \\ & - Losses\ of\ the\ absorber\ to\ the\ environment \end{aligned} \tag{5-2}$$

The solar irradiance reaching the collector, its aperture area, is calculated using the area of collector, the DNI (G_{SC}) and the cosines of the angle of incidence, see equation (5-3).

$$solar\ irradiance\ reaching\ the\ collector = Area_{collector} \cdot DNI \cdot \cos\theta_i \tag{5-3}$$

The percentage of the irradiance intercepted by the receiver is what it is usually referred to as the collector optical efficiency. It is calculated based on an angle of incidence $\theta_i = 0º$ and then multiplied by a factor which summarises the losses due to $\theta_i > 0º$, called Incidence Angle Modifier (IAM). Therefore, the optical performance can be calculated as in equation (5-4) :

$$\eta_{optical} = \eta_{optical,0^\circ} \cdot IAM(\theta_i) \tag{5-4}$$

The optical performance at 0º of a collector is defined in equation (5-5):

$$\eta_{optical,0^\circ} = \rho \cdot \gamma \cdot \tau \cdot \alpha \tag{5-5}$$

Being γ the intercept factor of the absorber, τ the transmittance of the absorber cover, for instance, a glass envelope in a PTC and α the absorptance of the solar receiver. All these operands change their value over time.

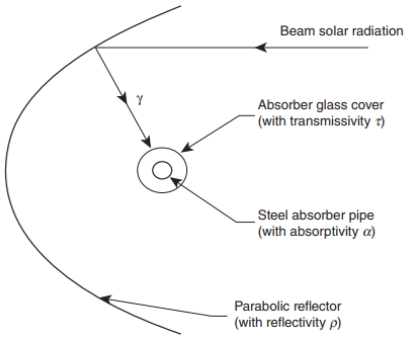

Figure 5-1 Optical losses in a PTC (Stein, 2012)

For the calculation of energy losses in a Heat Collector Element (HCE), the works of Bendt and Rabl [24] [68] describes the formulation to model them. Therefore, summarising the above-described equations into one single formula, the power absorbed in a PTC by the HTF can be simplified in equation (5-6)[9]:

$$\begin{aligned} Q_{net} = Area_{collector} \cdot DNI \cdot \cos\theta_i \cdot \rho_{specular} \cdot \gamma \cdot \tau \cdot \alpha \cdot IAM(\theta_i) \\ - \ Losses\ of\ the\ absorber\ to\ the\ environment \end{aligned} \tag{5-6}$$

Several authors [69] include a list of factors to consider the losses due to end losses, shadowing and the soiling in the collector. End losses and shadowing can be included in the Incidence Angle Modifier parameter since both are dependent on the angle of incidence. Since soiling produces scattering, this phenomenon will affect the specularity of the mirror. The effect soiling produces in the loss of reflectance of a collector can be included in the so-called cleanliness factor. This factor is calculated as the ratio between the average specular reflectance of the collector in operation and the nominal specular reflectance when the mirror is cleaned. All these factors (IAM, cleanliness, etc) reduce the power absorbed by the

[9] The definition of this formulae must be adapted for each CSP case, the equation here described is more suitable for PTC applications but can be adapted for CSR or dish systems too.

receiver in proportion to its value, so the relationship between power loss and these factors is directly proportional [68].

For CSP applications, the incidence angle is key for the optical performance in a collector [70] [71] [72]. The optical performance of a collector decreases with larger incidences angles, as can be seen in Figure 5-2 for a PTC:

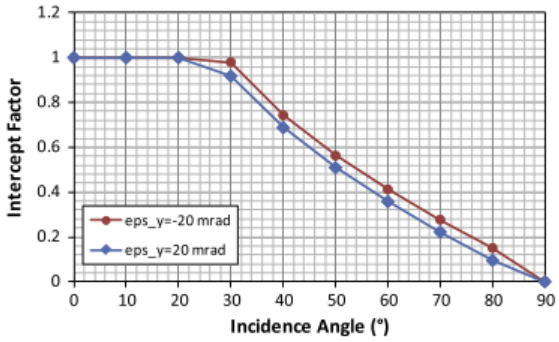

Figure 5-2 Intercept factor as a function of the incidence angle with only a constant ± 20 mrad longitudinal slope error in a LS2 PTC (Binotti et al., 2013)

Therefore, the incidence angle is a key parameter for designing efficient solar fields, not just because affect the mirror reflectance, but the collector itself.

5.2 Sources of errors leading to the loss of the reflectance

The type of potential errors that might be encountered in a mirror for concentrated solar purposes can be categorised in 3 main groups [35]:

- Due to the material (optical errors): specularity of the reflective material, roughness, dust film growth over the surface.
- Due to the manufacturing and assembly of the collector (geometrical errors): local slope errors, profile errors, misalignment of the reflector during assembly, mislocation of the absorber. See Figure 5-3.
- Due to the operation: Tracking issues, profile errors due to weathering.

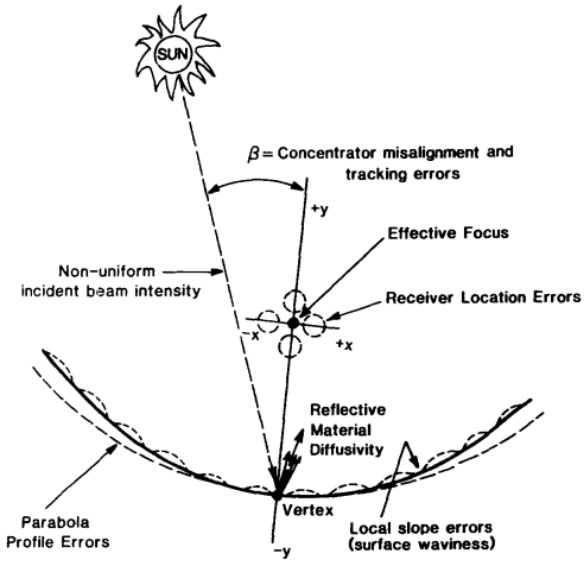

Figure 5-3 Description of potential geometrical and optical errors in a PTC (Güven and Bannerot, 1986)

There is a relationship between the source of the potential error and its dependency with the optical performance, see Figure 5-4.

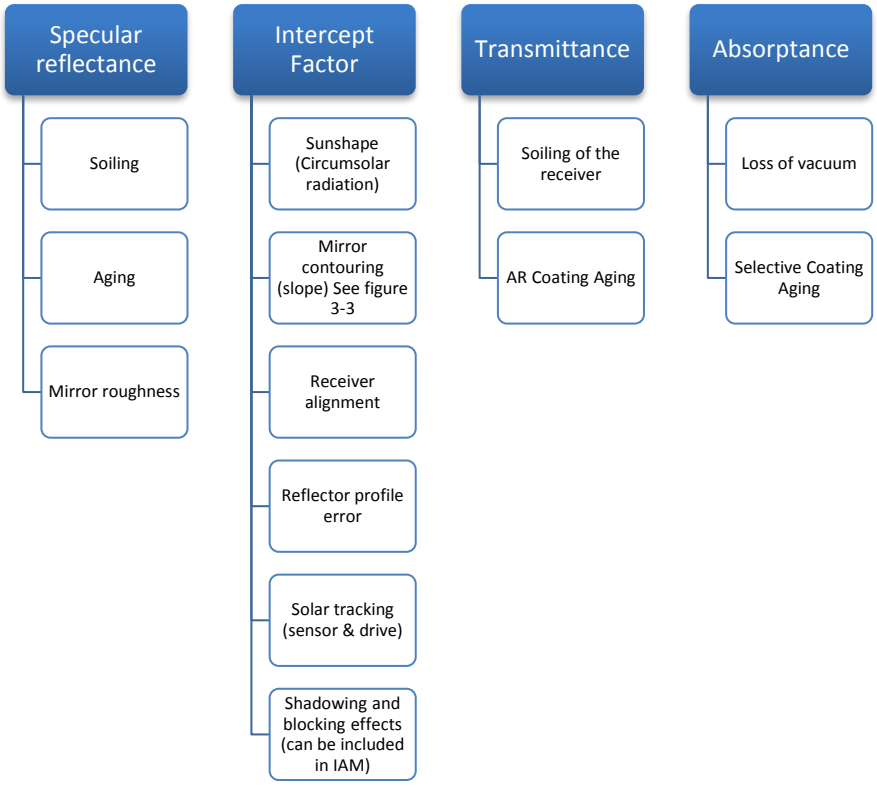

Figure 5-4 Root causes of loss of optical performance in a concentrator applied to a PTC

The specular reflectance is mainly lost due to issues with the reflective material, like aging and due to problems associated with the surface of the mirror and its intrinsic properties: roughness and soiling. The phenomena involved in the aging of a mirror could be listed as chemical corrosion, erosion (scratches due to dust), abrasion (scratches due to washing), solarization, delamination (layer bonding issues), UV degradation, layer cracking

(due to thermal stress) and tarnishing (degradation of the silver due to high temperatures). Those are factors affecting the durability of the reflector.

The intercept factor is influenced by quality problems in the manufacturing and assembly of the concentrator, involves all geometrical problems associated with the collector. They include reflector profile errors, consistent misalignment of the collector with the sun, and misalignment of the receiver with the effective focus of the sun (this problem is neglectable for a solar tower since the deviations in the design can be compensated by an offset in the heliostats), all problems which can be addressed implementing appropriate quality controls on site.

The operation of the plant can influence both specular reflectance and intercept factor. The quality of the tracking instruments installed, and the experience of skilled workers play a significant role.

The atmospheric conditions influence all parameters equally. For instance, high atmospheric humidity will absorb DNI (G_{SC}) and also reduces the reflectance of the mirrors due to condensation over the first layer. A sandstorm will difficult the tracking of the collector and soil the surface of the reflectors.

In general terms, there are two mechanisms of losing reflectance in a mirror: by absorption of the radiation or by scattering (dispersion) [42]. For instance, mirror soiling leads to a loss of optical performance due to absorption and dispersion at the same time. The effect of mirror soiling must be well studied and known by the plant operators to better predict the yield of a solar field and be able to schedule efficiently the cleaning and washing operations of the mirrors. It has been reported a daily loss of 0.5% hemispherical reflectance on outdoor-exposed mirrors in commercial plants in operation [73]. The loss of specular reflectance due to soiling in a reflector could range from 14 % to 26 % after a few months and it varies considerably depending on the location of the plant.

The scattering produced by dust on the mirrors is strongly related to the location of the plant, therefore dust characterization is a mandatory task for the correct measurement of solar reflectance in the field [74]. For modelling the soiling in a solar plant (CSP or PV), please refer to Bellmann *et al.*, 2020 [75]. As a key performance indicator in a CSP plant, some authors defined the cleanliness factor, F_C as in equation (5-7):

$$F_C = \frac{\rho_{soiled,s,\varphi}(\lambda, \varphi, \theta_i)}{\rho_{clean,s,\varphi}(\lambda, \varphi, \theta_i)} \tag{5-7}$$

For using this concept in the solar field, for instance, for the TraCS instrument described in chapter 6.4.3.1, the cleanliness factor of a mirror can also be defined as in equation (5-8) [76]:

$$F_C\,(t) = \frac{DNI_{reflected,soiled}(t)}{calibration\ constant \cdot DNI_{sun}(t)} \tag{5-8}$$

Being the calibration constant, the averaged clean reflected DNI of a mirror in comparison with the DNI of the sun reaching the collector. The change of cleanliness over a defined time interval Δt is defined as the soiling rate $r_{s,dt}$. The soiling rate is always related to a specific reported time interval, being hourly and daily the typical

values. For a more graphical description about how soiling affects the reflectance in SSMs, see Figure 5-5. A Pfahl *et al.* did resume a list of soiling-rate measurement campaigns over the world, refer to [47].

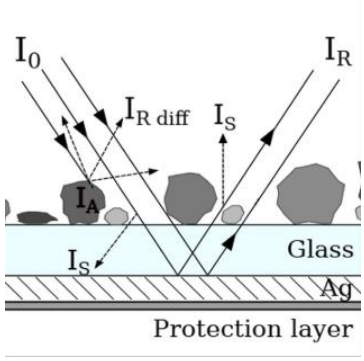

Figure 5-5 Interaction of irradiance with soiling particles on the surfaces of CSP mirrors (P. Bellmann, et al. 2020)

Regarding its randomness, errors can be categorised as random errors and non-random errors. Random errors are defined as those errors that are truly random in nature and can therefore be represented by normal (probability) distributions. These errors are identified as apparent changes in the width of the sun, scattering of defects associated with the optical material used in the reflector, and scattering effects caused by random local slope errors. Non-random errors are deterministic in nature. They account for the gross errors in manufacture/assembly and/or in operation. The non-random errors are identified as: concentrator profile errors, consistent misalignment of the trough with the sun, and misalignment of the receiver with the effective focus of the trough. The non-random errors can only be characterised to a Normal distribution if averaged over a large array of collectors or heliostats, or to include these errors as a factor to calculate a global intercept factor for the collector.

One of the advantages to define the reflectance as a sum of Gaussian functions is to be able to use these parameters such as standard deviation, in ray tracing models which calculate the intercept factor of an absorber or the performance of the plant giving the standard deviation of the collector or heliostat [77]. Then, optical errors can also be represented as a normal probability distribution. The total error in a concentrator is given as the sum of individual errors occurring in the system, as described in equation (5-9) [35]:

$$\sigma_{total}^2 = \sigma_{sun}^2 + (2\sigma)_{slope}^2 + \sigma_{tracking}^2 + \sigma_{mirror}^2 \tag{5-9}$$

Where σ_{sun} represents the standard deviation of the sun's energy distribution, σ_{slope} is the slope error distribution, $\sigma_{tracking}$ is the tracking error distribution and σ_{mirror} is the specularity error distribution.

According to Carlos Alcañiz *et al.* [37], the reflected profile (characterised as normal distributions) of the parabolic through configuration is different from a tower configuration and the tower setup is more sensible to non-specular behaviour in the reflectors than the PTC.

6 SOLAR REFLECTANCE MEASUREMENT

6.1 Characterization of the reflected beam profile of a mirror. Models for measuring the specular reflectance

Richard B. Pettit [12] [78] was one of the first and leading researchers to characterise the beam profile of reflected irradiation from a mirror for concentrated solar thermal purposes. His goal was to develop a method to characterise the properties of a mirror material independent of the characteristics of the measurement technique. He concluded that the radiation reflected would scatter the beam according to a normal distribution[10]. In later research, as previously mentioned, Richard B. Petit and J.M. Freese pointed out the wavelength dependence in the scattering phenomena.

6.1.1 Solar-weighted specular reflectance model

This model was developed by Pettit to ease the measurement of the averaged specular reflectance of a solar field, using portable available devices. Pettit proposed two assumptions:

1. The ratio between specular and hemispherical is wavelength-independent
2. If the first assumption is false, the second assumption is that the above-mentioned approximation leads to a small error compared with the averaged loss of reflectance in a mirror.

In that case, the following equation shall be used:

$$\rho_{s,\varphi}([\lambda_a,\lambda_b],\theta_i,\varphi] = \rho_{s,h}([\lambda_a,\lambda_b],\theta_i,h)\cdot\frac{\rho_{\lambda,\varphi}(\lambda_c,\theta_i,\varphi)}{\rho_{\lambda,h}(\lambda_c,\theta_i,h)}$$

In this equation, $\rho_{\lambda,\varphi}(\lambda_c,\theta_i,\varphi)$ is measured using a portable reflectometer and the solar-weighted hemispherical reflectance and the monochromatic hemispherical reflectance are measured by laboratory devices (spectrophotometer) before the installation of the mirror on the field. This model might be used for highly specular reflectors as the silvered second surface mirrors.

The solar-weighted specular reflectance can be calculated by multiplying $\rho_{s,h}$([280–2500] nm, 8°, h) by the ratio of $\rho_{\lambda,h}$ (660 nm, 8°, h) / $\rho_{\lambda,\varphi}$ (660 nm, 8°, 12.5 mrad), according to Pettit equation proposed in [12]. This calculation for determining the solar-weighted specular reflectance, which assumes that the ratio of specular to hemispherical reflectance at a certain λ (in this case at 660 nm) is constant over the whole solar spectrum, is widely accepted [41]. However, this assumption is only valid for highly specular reflectors such as silvered glass. Single wavelength measurements in multilayer mirrors might lead to large deviations of the calculated solar-weighted specular reflectance [37] [59]. As for the SSM, it can be assumed that scattering is essentially

[10] The relationship between surface roughness, which is present in all the reflectance cases, and the scattering of the reflected light was first described by H. Davies, 1954 in his work "The reflection of electromagnetic waves from a rough surface". Although Richard B. Pettit *et al.* were the ones to develop techniques to apply such research to the solar field.

independent of wavelength over the whole solar spectrum and that the beam has a Gaussian shape. However, it is well-known that these two conditions are not fulfilled after the aging tests due to scattering and absorption effects on the corroded reflector surface. Therefore, degradation of the reflective layer cannot be monitored by using this equation.

6.1.2 Spectral specular reflectance model with one and two Gaussian

The beam spread of a solar reflector (beam scattering) can be described by a model function with one Gaussian [12], see equation (6-1):

$$\rho_{\lambda,\varphi}(\lambda, \theta_i, \varphi] \propto \exp\left(\frac{-\Delta\varphi^2}{2\sigma^2}\right) \tag{6-1}$$

Where $\Delta\theta$ is the deviation of the reflected beam from the specular direction and σ is the standard deviation of the distribution. It is assumed that the average surface height and slope distribution can be characterised by a normal distribution. σ is wavelength dependant. This model is validated for material with low scattering and no dust over the tested surface.

However, for some materials like the roll-polished aluminium, the reflectance profile does not suit well by a single normal distribution. The reflectance profile of such materials can be characterised by the sum of two normal distributions, see equation (6-2) :

$$\rho_{\lambda,\varphi}(\lambda, \theta_i, \varphi] \propto \rho_1 \exp\left(\frac{-\Delta\varphi^2}{2{\sigma_1}^2}\right) + \rho_2 \exp\left(\frac{-\Delta\varphi^2}{2{\sigma_2}^2}\right) \tag{6-2}$$

For instance, for laminated plastic films, one distribution will refer to the intrinsic properties of metallized plastic film and the other one will refer to the scattering due to the bonding interface.

With these two models, it can be covered most of the commercial reflective surfaces. There are more reflectance models in the bibliography, please refer to [76] for a detailed list.

There are more techniques used for the characterization of reflective surfaces of solar concentrators, please refer to Arancibia-Bulnes *et al.* [77] for a more detailed view of the methods developed to characterise the peculiarities of reflectance profile of a mirror.

6.2 Equipment to measure solar radiation

The instruments for measuring solar radiation are generally of two types: pyranometers, see Figure 6-1, which accept radiation from the entire hemisphere, and pyrheliometers, see Figure 6-2, which accept radiation from only one direction (more precisely from a cone of 2.8° half-angle). The pyranometer measures hemispherical insolation (GHI), while the pyrheliometer measures the beam component of the insolation (DNI or G_{SC}). Both pyranometer and pyrheliometer operate on the principle of measuring the temperature rise of a black absorber as it is heated by the sun. These devices with adaptations can be used in the field to evaluate the dust accumulation on the mirrors or the current soiling rate.

Figure 6-1 CMP3 second class pyranometer - Kipp & Zonen

Figure 6-2 DN5 First Class Pyrheliometer - Middleton Solar

6.3 Equipment to measure solar reflectance

The difficulty in measuring solar reflectance lies in the broad parameter range influencing the reflectance of a mirror employed in CSP. The evaluation of the quality of a reflector involves most of the solar spectral wavelength range, an incidence angle from near normal up to 70º and a very narrow acceptance angle from near specular to around 20 mrad. To measure reflectance spectrophotometers and reflectometers are usually used.

6.3.1 Spectrophotometers

A spectrophotometer is a photometer (a device for measuring light intensity) that can measure intensity as a function of the light source wavelength λ. The main advantage of a spectrophotometer for solar applications is the fact that the reflectance can be measured over the entire solar spectral range, UV, VIS and NIR, with the use of one or dual light sources and monochromators. See Figure 6-3 for a schematic plan of a typical spectrophotometer.

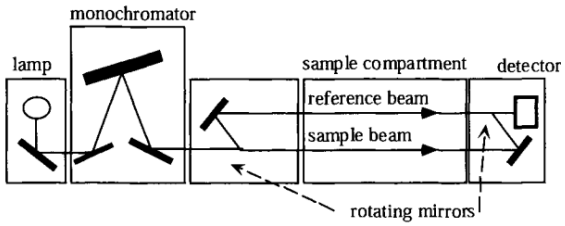

Figure 6-3 Schematic plan of a typical spectrophotometer (Ross, 2004)

For the case of solar applications, it is extensively used in laboratories with integrating spheres (see Figure 6-4) for evaluation of the hemispherical, diffuse and (as a difference of both) specular reflectance. Diffuse reflectance is measured by directing the specular reflected beam through a sphere opening (light trap). Thus, in the sphere, only the diffusely reflected light is detected.

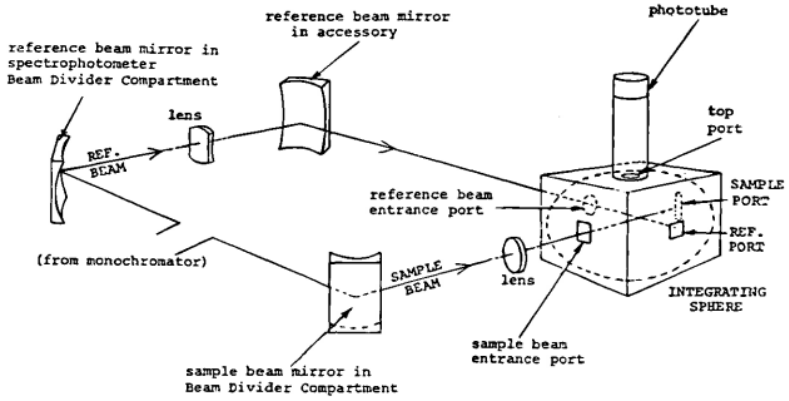

Figure 6-4 Type I illumination system with an integrating sphere from a Cary Spectrophotometer Model 1711 (Murray, 1998)

The major disadvantage of this kind of equipment is that it is not portable. So, its use is restricted to laboratories only. Besides, in general, the adjustment of the acceptance angle for the measurement of specular reflectance is not possible. Additionally, the usual angle of incidence of these devices ranges from $8º < \theta_i < 15º$ and measuring curved mirrors leads to errors in the measured value. For CSP purposes, the are several accessories to help to characterize a mirror. For instance, the Universal Reflectance Accessory (URA) by Perkin Elmer [76] is used to measure specular reflectance at larger incidence angles than in an integrating sphere, being able to detect scattering of the material due to degradation. However, as the acceptance angle is larger than the required in concentrating solar thermal technologies, its use is not widely extended. To meet this need, Montecchi proposed

a single experimental device disposition using though an integrating sphere for measuring near-specular and hemispherical reflectance at semi-acceptance-angles suitable for CSP applications [79].

As a list of spectrophotometers used for solar applications, there are many:

- Lambda 950/1050 by Perkin Elmer
- Cary 5000 by Agilent (formerly Varian)
- OL 750 by Gooch and Housego (formerly Optronic laboratories)
- V670 by Jasco

A more detailed description of these devices and its characteristics can be found in [76]. The influencing factors for measuring solar reflectance using spectrophotometers with integrating spheres can be listed in:

- The spectral bandwidth of the light source
- Accuracy of measurement
- The mirror used as a reference standard (or coupon)
- Size and opening of integrating sphere
- Size of the reflected beam
- Size of the light trap for diffuse measurements

6.3.2 Reflectometers

Reflectometers measure the intensity of the light source after reflection on a sample. They are equipped with light sources that radiate only one or a few narrow wavelength lines or bands, so they give less information about the broad spreading of the reflected light than spectrophotometers. These lines or bands should at least be near the solar energy peak between λ = 500 nm and λ = 660 nm (see Figure 3-6). They must always be calibrated with a known reference standard, since the device measures the flux in the sample and compare it with the calibrated one, hence giving a relative reflectance value. These are used in the field to quantify the cleanliness factor (see chapters 5.2 and 6.4.3). The beam alignment for each measurement should be adjustable to compensate for any surface curvatures. The positioning adjustment should be stable without damaging the mirror. It has been told several times during this work that the scattering phenomenon is wavelength-dependent and that relationship is stronger if the quality of the mirror material is poor and there is dust over the sample surface, therefore, the reflectometers designed to be used in the field must have as a feature the possibility to measure at different wavelengths, as broad as possible is desirable, but in the range of the VIS is recommended. The lamps used for the generation of the sample light is never monochromatic, it has to pass through several filters to modify its wave spectral distribution, so the quality of the lamps used is also a critical point in the design of such devices. The near-specular reflectance is only interesting to calculate for CSP purposes (see chapter 3.3.2), so at least the acceptance angle should have a range between 7.5 mrads and 23 mrads.

Both types of equipment (spectrophotometers and reflectometers) use detectors to measure the reflected beam from the sample. Detectors are devices which convert the useful information carried in electromagnetic waves into forms which can be more easily handled and interpreted. The ideal detector properties can be summarized as follows [80]:

- Wide wavelength range
- Highly sensitive
- High signal-to-noise ratio
- Reacts immediately to changes in the incoming signal
- Produces a linear response which is independent of wavelength
- Durable and stable over time

For example, a list of detectors and its useful detection range is presented in Table 6-1.

Table 6-1 UV-VIS, NIR, and IR Detectors [81]

	Useful detection range
Detector type	μm
Silicon	0.30 - 1.10
PbS	1.1 - 3.0
InAs	1.7 - 5.7
InGaAs	0.90 - 1.7
Ge : X	2 – 40
Ge : Au	2 – 9
Ge : Cd	2 – 24
PbSe	1.7 – 5.5
Ge : Zn	2 – 40
InSb	1.8 – 6.8

	Useful detection range
Detector type	μm
PbTe	1.5 – 4.5
MCT (photovoltaic)	1 – 17
TGS (triglycine sulfate)	10 – 120
HgCdTe	1.5 – 16
PLT (pyroelectric lithium tantalate)	1.5 – 30

For a better understanding of the characteristics and limits of the equipment used to measure reflectance, the parameters which measure the performance of a detector can be condensed in:

1. Responsivity (as photosensitivity)
2. Spectral response
3. Response time
4. Time-constant
5. Cut-off frequency
6. Noise Equivalent Power
7. Detectivity
8. Dynamic Range

6.4 Reflectance measurement in the field[11]

6.4.1 Methods and procedures

The main goal to measure reflectance for an O&M department is to evaluate the aging of the reflector material[12] and optimize the mirror washing schedules in the plant. Soiling induces losses 8 -14 times greater for CSP plants than in a PV plant [75] since the scattered light can not be used in STE plants. It is recommended to create and validate a model to find a correlation between cleanliness or soiling rate and plant energy yield, to separate the

[11] For the standard equipment used in laboratory to characterize the reflectance spectra of mirrors, please refer to [74].
[12] The reflectance measurement also gives valuable information about the quality of the reflector material and its construction, in case of multilayer reflectors. But this characterisation must be performed either by the manufacturer or by the constructor or owner before the installation of the mirror in the field.

prediction of the plant energy yield from the measure of reflectance on the field.

For the state-of-the-art methods and procedures of how to measure reflectance, the reader should go to the work published by the Task III of the SolarPACES organization [14] [16] and to the individual work published by the researchers belonging to the Task III group. This group has been working at an international level for almost 10 years on the standardization of reflectance measurements and so far, they have focused on standardizing procedures for the measurement of reflectance in the laboratory. In March 2018 they published the 3rd version of its official reflectance guideline, where they have included some simplified method of measuring soiled and/or aged reflectors. Currently (October 2019), they have started a new project to advance in the standardization of reflectance measurements in the field. A list of hints will be given in this work:

1. Hemispherical reflectance on the field is not possible to be measured, leave that task for a laboratory in clean and controlled conditions, with advanced equipment.
2. To monitor the aging, till more advance equipment and techniques are developed, it is sufficient to measure the specular reflectance at one defined wavelength in the range $\lambda = [400, 700]$ nm, $\theta_i \leq 15º$ and a $\varphi \leq 20$ mrads. But this is a simplification due to the lack of technology to accurately measure the aging of a reflector.
3. The beam spot size of the device shall be selected according to what it is needed to measure. A bigger spot size will cover more defects on the surface, leading to a representative measure of the total surface of a facet, for instance, but it will also produce more scattering, leading to loss of specularity in the value obtained. Thus, depending on what it is needed to be characterized (soiling, aging), the beam spot size shall be selected accordingly.
4. The area of the aperture of the detector must be adjustable for specular measurement, having at least an acceptance area of $\varphi \leq 20$ mrads.
5. Devices must be warmed up before the use, instruments usually have a temperature coefficient % / ºC.
6. Measurement of the reflectance must be carried out by an expert technician. Training by the engineering department or R&D department is mandatory as it is demonstrated that the measurement is operator dependant [76].
7. A standard reference for calibration before use is necessary, mandatory in the use of reflectometers which are not able to measure absolute reflectance. Always keep in a safe place and clean the reference in the field. If the reference gets dirty, the accuracy and repeatability of the measures will differ from one heliostat to another or from one measure to another. If possible, use reflectometers which can be calibrated after several measurements.
8. Use reflectometers which have some kind of automatization of the measurement or delay after pushing the “GO” buttons to take the measurement as still as possible.

9. Preferably, the device shall give the option to measure with no or slight contact to the surface.
10. Adjustment options for different mirror thicknesses and surface curvature is a must.
11. During the measurement, the equipment shall be designed to not to be influenced by the external light.
12. Minimum type-B1 uncertainties.
13. Ergonomic design: lightweight, large autonomy, easy handling, screen back-illuminated.

Above all, the use of reflectometers or reflectance measurement devices in the field imply a high effort and human-resource allocation. The goal for lower OPEX is searching for an automated system to measure overall reflectance and cleanliness for your type of CSP plant. Integrated sensors with autonomous mode and Internet of Things (IoT) capabilities, models validated with machine learnings techniques, use of drones, will help lower the OPEX and predicting and enhance control of the plant energy output.

6.4.2 Commercial devices

Commercial equipment on the market for measuring reflectance on the field can be grouped according to the reflectance that is best suited to measure: hemispherical or specular. The differences between them are that the hemispherical instruments are sphere-type spectrophotometers which calculate the specular reflectance subtracting the diffuse reflectance from the hemispherical reflectance. Table 6-2 contains a list of devices suitable for measuring reflectance or soiling in outdoors.

Table 6-2 List of commercial devices for measuring reflectance or soiling in outdoors

Type of reflectometer	Manufacturer	Model
Hemispherical[13]	Surface Optics	410 Solar
Hemispherical	Konica Minolta	CM-700d/600d
Specular	Devices & Services	15R-USB / 15R-RGB
Specular	Schmitt Measurement Systems	μScan[14]
Specular[15]	Aragon Photonics and Abengoa Solar	Condor

[13] The SOC-410 measures total, diffuse and specular reflectance but with a $\varphi = 52.4$ mrad, too large acceptance angle for measuring specular reflectance for CSP applications.
[14] According to work performed at CIEMAT-PSA [86] it is not suitable for high quality CSP reflector characterization.
[15] Condor $\varphi = 290$ mrad, too large acceptance angle for measuring specular reflectance for CSP applications. Larger acceptance angles on portable reflectometers avoid to proper characterise the soiling effect on the mirror.

Type of reflectometer	Manufacturer	Model
Specular	PSE AG and Fraunhofer Institute for Solar Energy Systems	PFlex
For soiling purposes	CSP Services GbmH	TraCS
For soiling purposes	Fraunhofer Institute for Solar Energy Systems	AVUS
For soiling purposes	IK4-Tekniker and RIOGLASS SOLAR	SMARTMIRROR

Concerning to reflectometers, it might be mentioned that the equipment based on an integrating sphere that measures hemispherical and diffuse reflectance (410 Solar by Surface Optics and CM-700d/600d by Konica Minolta) is not widely used in CSP plants, with some exceptions such as BrightSource company which is measuring reflectance on the field with the Konica Minolta device. On the contrary, the device more widely used is the portable specular reflectometer D&S 15R by Devices & Services. This equipment was developed by the company in cooperation with Sandia National Laboratories (USA) at the beginning of the eighties of the last century. It presents a very high accuracy because it can measure at several acceptance angles which are suitable for CSP applications (7.5, 12.5 and 23 mrad) and is the preferred one for research purposes. Nevertheless, it suffers from several drawbacks for regular measurements in the field because the calibration process requires time and experience. Besides, the 15R is a monochromatic device and the multi-wavelength version (15R-RGB) implies a calibration process every time that the wavelength is changed, which is a time consuming and consequently non-practical task. The Condor reflectometer was born with the main philosophy of avoiding the practical issues linked to the D&S 15R. It was developed by Abengoa and the University of Zaragoza, and Aragón Photonics commercially distributes it since 2012 worldwide [82]. In comparison with the D&S 15R, it is much more practical because the calibration process and data storage are much easier, and it can measure at several wavelengths without additional calibration. However, its acceptance angle is much wider than the D&S one (290 mrad). Finally, the PFlex was created with features in between of the two previous equipment, presenting some of the advantages of the Condor, but with a smaller acceptance angle (74 mrad). The D&S 15R, PFlex and the Condor can measure in curved mirrors, fast and without being influenced by the external light.

As a general comment, the use of reflectometers should be limited to validate other more agile and automatic configurations that measure reflectance (such as the AVUS or SMARTMIRROR) in the field or to validate energy yield calculation models by measuring other parameters such as soiling rate.

6.4.3 Commercial devices for soiling measuring

The use of soiling devices in the commercial CSP plants are soaring due to the direct correlation between soiling

and annual gross electrical yield. The importance of an accurate prediction of the soiling rate lies in the bankability of the plant and its feasibility. Measuring accurate and precise values of soiling rate leads to an optimized cleaning process, better predictions on energy yield and less LCOE in general. A brief description of the main soiling devices is presented.

6.4.3.1 TraCS developed by CSP Services and the Deutsches Zentrum für Luft- und Raumfahrt (DLR)

The TraCS (Tracking Cleanliness Sensor) is an accessory for a fixed based meteorological station, in this case, is a Solys2 tracker manufactured by Kipp&Zonen [74]. Developed by the DLR and commercialised by CSP Services, a spin-off of the DLR. The station consists of four measurement devices: Two pyranometers for measuring Diffuse and Global Irradiance (DHI and GHI) and two pyrheliometers for measuring the DNI of the sun and the reflected DNI of the mirror sample. The pyrheliometers used are from Kipp&Zonen models CHP1 and CH1, both are thermopile sensors. One of the pyranometers is facing directly to the sun (Figure 6-5, right) while the other one is mounted facing down looking to the mirror sample (Figure 6-5, left)

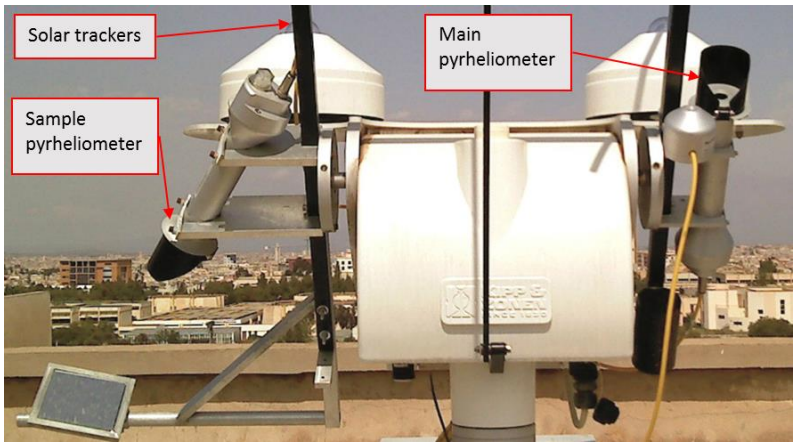

Figure 6-5 A meteorological station with main and TraCS pyrheliometer

A major advantage of this equipment is that it can measure absolute reflectance in real-time and automatically, and even short-term changes in the cleanliness can be detected. To obtain a reflectance value, it simply divides the value obtained by the main pyrheliometer by the value obtained by the TraCS pyrheliometer. This value is obtained with the current DNI of the sun at the moment of the measurement. To be able to measure any kind of mirror used in CSP, it is used as a constant calibration factor or "cleanliness factor".

In comparison with the D&S 15R portable reflectometer, the TraCS setup overestimates the cleanliness. It may be caused by the different measurement spectra used by both detectors or by the viewing field of the D&S's detector, which is larger than its measurement spot, resulting in less light being scattered into the optics and giving a lower value than the TraCS pyrheliometer. The precision (precision, in this case, is measuring a larger area size in which more imperfections could be measured) of the TraCS is better than with a portable reflectometer due to a larger measurement spot.

6.4.3.2 AVUS developed by Fraunhofer Institute for Solar Energy Systems

The AVUS measurement device directly measures reflectance and cleanliness of the solar field in an automatic

mode [83]. The soiling rate can be calculated as well since the device offers the possibility to set up an automatic sample measurement at an hourly or daily basis. Data can be collected in real-time thanks to the UMTS modem connected to the device. The device can be attached to a meteorological station or as an independent device. Its main characteristics are:

- As a detector, uses an integrated sphere with a Silicon detector, with a LED illumination with a red light at $\lambda = 660$ nm and a nominal acceptance half-angle $\varphi = 51$ mrad
- Reflectance and cleanliness data for acceptance half angles of 51 mrad, 7.5 mrad, 12.5 mrad and 23mrad
- The default tilt angle of exposed mirror samples 30°, optional angles of 45°, 60°, 75°
- Accuracy of cleanliness and reflectance: Resolution of 0.001 and repeatability of ± 0.005

It stores several sample mirrors to increase its maintenance period, once a sample has reached its maximum soiling, this is stored inside the device and a new cleaned sample is deployed. This device has proven to measure reliable soiling rates as it is demonstrated in a pilot test in a PTC plant in south Spain (see Figure 6-6). Three AVUS instruments showed a mean deviation of 0.16 % and a standard deviation of 0.34 %.

Figure 6-6 AVUS instrument prototypes for automated in-situ soiling rates and cleanliness (Heimsath, 2018)

6.4.3.3 SMARTMIRROR developed by IK4-Tekniker and RIOGLASS SOLAR

IK4-Tekniker started developed this new sensor set-up back in 2013 [84]. It is based in photodiodes detectors gathering the light scattering radiation from a transparent substrate that is exposed to the same environment as the mirrors and located next to them (see Figure 6-7 and Figure 6-8).

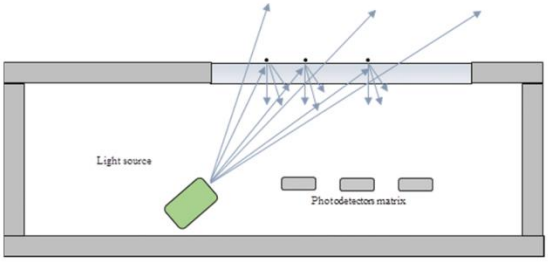

Figure 6-7 IK4-Tekniker 2013 prototype, scheme of the soiling sensor (Fernández García et al., 2017)

Figure 6-8 IK4-Tekniker 2013 prototype attached to a heliostat in the CESA installations from CIEMAT-PSA (Calvo, et al. 2018)

In the last years, IK4-Tekniker has associated with RIOGLASS SOLAR for the creation of more robust and improved hardware ready to be deployed in the field or installed in a mirror. The consequence of this association is the generation of patent No. WO2018069558-A1. The developed device is called SMARTMIRROR [85], and it is proposed to be installed in the mirror in two configurations: as a black box integrated into the mirror structure or as a naked sensor to be incorporated to the back of the mirror using the mirror glass layer as protection. 30 prototypes of the black box version are planned to be tested in the CSP plant "La Africana" in south Spain. After the evaluation process is done, the results will be compared with a reflectance measurement campaign with reflectometers to validate the equipment. As advantages, this setup offers real-time monitoring of the soiling condition of the plant, reducing the need of extra manpower for the operation of the plant and can be incorporated directly in the mirror layer itself, the RIOGLASS participation in the development of such devices gives stability and trust to the project. This device has been developed within the framework of the European project SOLWARIS, which aims to solve water issues for CSP plants, see [86].

Figure 6-9 SMARTMIRROR black box configuration. Left: Sensor 3D design. Centre: Sensor integrated into a mirror. Right: 30 sensors manufactured and assembled; ready to be integrated into the mirrors at the site (La Africana) (Calvo et al., 2020)

6.4.4 Determination of the mean reflectance of a solar field in operation

For any proposed model to calculate straight-forward the current mean reflectance of a solar field, the number of measurements to be taken and the validation of the method are two fundamental steps to give credibility to the proposed model. The goal of statistical analysis is to identify some criteria for finding the mean reflectance of a heliostat solar field and its possible source of variations. According to Fernández-Reche [87], three criteria can be identified:

1. the position of the measurement in the facet
2. the facet position in the heliostat
3. the focal group in the solar field.

The statistical analysis (it can be applied for CSP reflectors too, please refer to Fernández García [88]) will conclude if it could be measured in any position of the facet or some particular position reveals more information about reflectance than others. And the same goes for the other possible sources. For the first two sources of variations, the statistical analysis is performed through an ANOVA analysis of variance. Before doing that, one of the assumptions in the ANOVA is that the probability distribution of the responses must be normal or fit in a normal distribution. So, a test of normality must be performed to perform the ANOVA with the raw data. Otherwise, the data would have to be normalized. All the ANOVA analysis must be performed with a significance level of 95%.

To determine if there are one single group of heliostats or more in the solar field, without considering its focal length, a cluster analysis is more appropriated. In the case that the field heliostats would be clusterised, it will require to measure representative heliostats for each cluster, making the task more time-consuming. One reason why this can happen is that there are heliostats that get dirtier than others in the solar field.

In the study of Fernández-Reche, the statistical analysis shows that there is no significant variation in the position of the measurement on the facet, neither was a significant difference between the facets in the heliostats. From the cluster analysis, two groups were defined, but it was related to the dirtiness of two heliostats which could not be washed while the others were, so if the soiling factor is homogeneous in all the field, all the heliostats can be grouped regardless of where they are located in the solar field. Therefore, the plant operator could select the easiest point in the facet to perform the measurement and the more accessible facet to do it. To select a representative sample, Fernández-Reche uses the following formula:

$$n = \frac{1}{\frac{E^2}{k^2 \cdot S^2} + \frac{1}{N}}$$

Where n is the size of the sample, N the sample population, E the error associated with the process, k a factor associated with the significance level and S^2 is the sample variance. The parameters in this equation which are variables are n and E. So, if an error is defined, several heliostats have to be sampled to obtain this error. The

total error of the measurement then is the sum of the statistical error of the process and the error associated with the measurement device. In the case that the null hypothesis of the ANOVA analysis cannot be accepted, other post hoc tests might be performed. Fernández-Reche recommends Tukey test [89].

For the validation of this method, a measurement campaign has to be carried out after agreeing on the measurement procedure, as said, position in the facet, facet position in the heliostat and heliostat clusters. The campaign has to be long enough in time to cover all the environmental and maintenance situations given in real life. At the same time, sufficient measurement data must be collected to ensure that the total procedural error is less than 0,3%. The collected data from the campaign could be used in a heliostat field simulation software, to obtain a total power coming from the field. That value could be then compared with solar flux measurements done in the receptor itself through a flux mapping system like the proHERMES developed by the DLR.

As an example, the data measured with the proHERMES-2A in the receptor and the given by a heliostat simulation software differs between 1.9% and 2.2%. Having both methods almost same error in calculating the total power in kW.

6.5 Ishikawa Diagram: Reflectance measurement

To summarize all the factors involved in the measurement of the reflectance in solar thermal power plants, an Ishikawa diagram or Fishbone diagram has been created. The problem here describe is the reflectance measurement in a mirror. The Ishikawa diagram categorizes the sources of errors in 6 categories: Materials, Method - Procedure, Environmental - Location, Operator, Measurement and Machine.

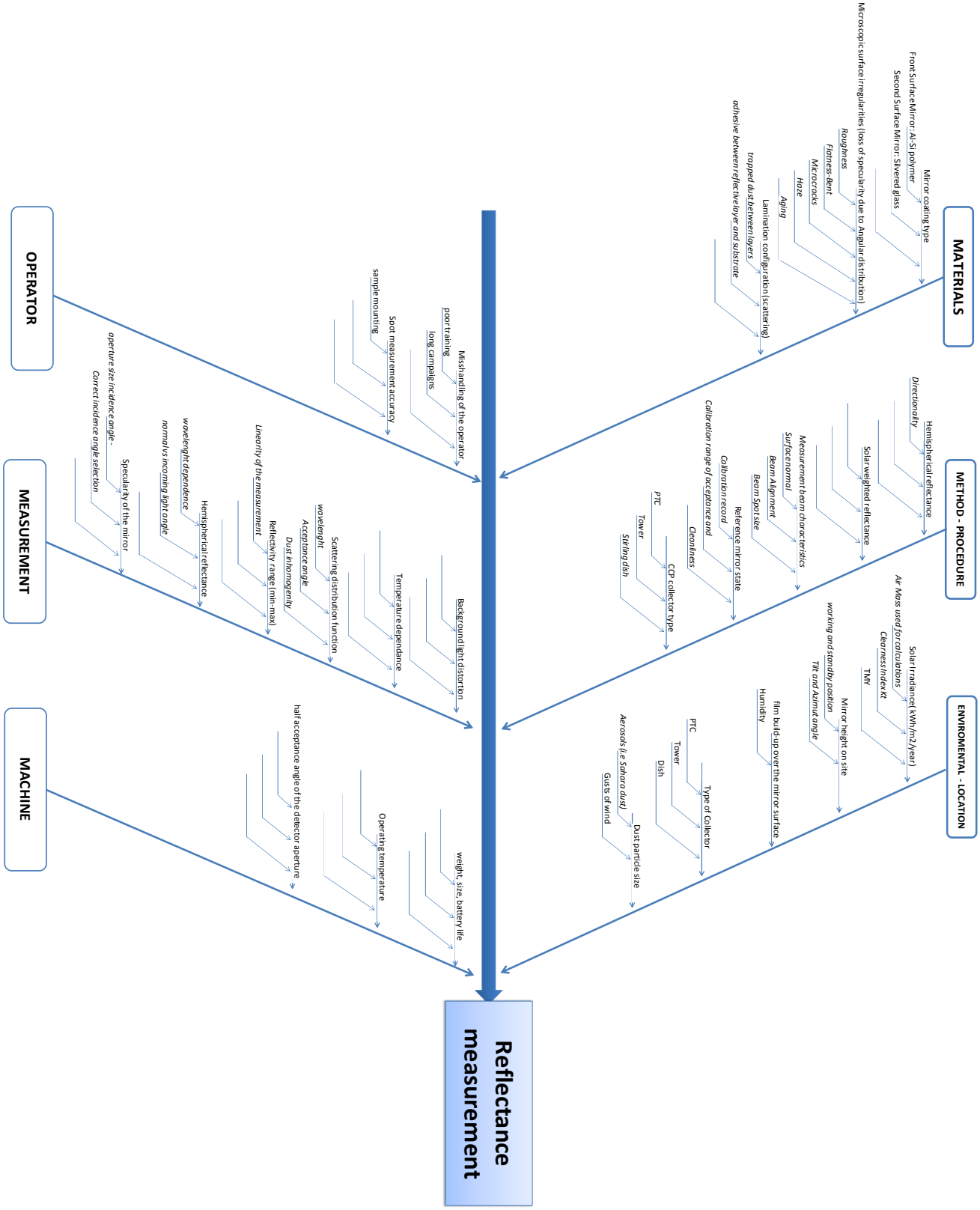

Figure 6-10 Ishikawa diagram: reflectance measurement

7 CONCLUSIONS

The characterization of the reflectance beam profile on any material has been researched during the past 70 years, reaching a very mature status about the procedures, equipment, and knowledge about how to measure reflectance in a reflective surface and how to characterise its sources of errors.

However, the measuring of the condition of the solar field (aging, soiling), regarding mirrors, is still a very time-consuming and expensive task for any plant operators. The portable reflectance devices have been developed over the past 40 years without many notable advances. The list of portable devices manufacturers is short, and no device stands out from the rest, meaning that the measurement of reflectance in the field by portable devices could not be the solution to measure the overall condition of a heliostat/collector field regularly. These campaigns are expensive in manpower and in time, and the data collected is not always accurate since the portable devices are not user friendly. Any model proposed to measure in near-real-time the average reflectance value of a plant should not include such continuous campaigns where the operators, which should always be properly trained for that task, measure reflectance with portable devices in the field. More research effort is needed to eliminate portable equipment and that these are only used for specific measurements to validate the results of other more advanced and less labour-intensive methods: the idea of installing sensors in the mirror such as the SMARTMIRROR, the idea of the AVUS, using devices with IoT capabilities or drones (there are research centres such as DLR, CIEMAT and ENEA working on this issue) should be the lines of action of research centres. Sadly, most of the advances and research in the reflectance field have come the above-mentioned research centres. Initiatives like the SOLWARIS project [86], funded by the European Union, help to maintain the progress in solving the biggest problems STE plants are facing. Although this project aims to reduce the water consumption in a CSP plant, measure reflectance as a relative measure when measuring soiling could help to develop the equipment and procedures to assess the overall condition of the solar field in an agile manner.

In the past years, the bankruptcy of several mirror manufacturers did not help in the search for better mirror setups. AET and OET performed in the most common used mirror setups have shown that there is still work to do to achieve a high reflectance profile over the lifetime of an STE plant. As well, it seems that all the progress from new mirror materials and configuration is coming from the research centres and the private sector is no investing more funds in such tasks. The low integration of STE plants in the grid systems all over the world might induce the constructors not to invest money in technologies with high LCOE. However, it has been demonstrated that in order to have a high integration of renewable systems into the electricity grid, it is necessary to integrate systems with high availability and high-capacity factors into the grid, and in this case, CSP technology is the only mature technology that offers dispatchability of power generation at low risk.

Finally, the new era of the 5G communications is going to ease the use of drones and the implementation of IoT devices in the energy plants. A revision of how these new devices can help to reduce the LCOE of a CSP plant might be helpful in the coming future.

CONCLUSIONES

La caracterización del perfil de reflectancia de los materiales con características reflectantes se lleva investigando desde hace más de 60 años, habiendo alcanzado este aspecto una madurez en cuanto a los procedimientos, los equipos de medida y el progreso sobre cómo medir la reflectancia en una superficie reflectante y cómo caracterizar sus errores.

Sin embargo, la medición del estado del campo solar (envejecimiento, suciedad), en lo que respecta a los espejos, sigue siendo una tarea muy lenta y costosa para cualquier operador de planta. Los dispositivos portátiles de reflectancia se han desarrollado en los últimos 40 años sin muchos avances notables. La lista de fabricantes de dispositivos portátiles es corta y ningún dispositivo se destaca del resto, lo que significa que la medición de la reflectancia en el campo mediante dispositivos portátiles no podría ser la solución para medir el estado general de un campo de helióstatos/colectores con regularidad. Estas campañas de testeo son costosas en mano de obra y en tiempo, y los datos recogidos no siempre son precisos, ya que los dispositivos portátiles no son fáciles de usar. Cualquier modelo propuesto para medir en tiempo casi real el valor medio de reflectancia de una planta no debería incluir esas campañas continuas en las que los operadores, que siempre deberían estar debidamente capacitados para esa tarea, miden la reflectancia con dispositivos portátiles sobre el terreno. Es necesario un mayor esfuerzo de investigación para eliminar los equipos portátiles y que éstos sólo se utilicen para mediciones específicas para validar los resultados de otros métodos más avanzados y menos intensivos en mano de obra: la idea de instalar sensores en el espejo como el SMARTMIRROR, la idea del dispositivo AVUS, utilizar dispositivos con capacidad de IoT o drones (hay centros de investigación como el DLR, el CIEMAT y el ENEA que trabajan en este tema) deberían ser las líneas de acción de los centros de investigación. Lamentablemente, la mayoría de los avances e investigaciones en el campo de la reflectancia han venido de los centros de investigación mencionados. Iniciativas como el proyecto SOLWARIS [86], financiado por la Unión Europea, ayudan a reducir los costes medioambientales y operativos de las plantas de energía de concentración. Aunque este proyecto tiene como objetivo reducir el consumo de agua en una planta de CSP, la medición de la reflectancia como medida relativa al medir la suciedad podría ayudar a desarrollar el equipo y los procedimientos para evaluar el estado general del campo solar de una manera ágil.

En los últimos años, la quiebra de varios fabricantes de espejos no ha ayudado en el desarrollo de mejores configuraciones de espejos o nuevos materiales. Los AET y OET realizados en las configuraciones de espejos más comunes han demostrado que todavía queda trabajo por hacer para lograr una configuración que mantenga una reflectancia especular alta durante la vida útil de la planta. Además, parece que todo el progreso de los nuevos materiales y configuraciones de espejos proviene de los centros de investigación y el sector privado no está invirtiendo más fondos en esas tareas. La escasa integración de las plantas CSP en los sistemas de red de todo el mundo podría inducir a los promotores de tales plantas a no invertir dinero en tecnologías de alto LCOE. No obstante, se ha demostrado que, para tener una alta integración de sistemas renovables en la red eléctrica, es necesario integrar en la red sistemas con alta disponibilidad y factores de capacidad altos, y en ese caso, la

tecnología CSP es la única tecnología madura que ofrece gestionabilidad de la generación de la energía a bajo riesgo.

Finalmente, la nueva era de las comunicaciones 5G va a facilitar el uso de drones y la implementación de dispositivos de IoT en las plantas de energía. Una revisión de cómo estos nuevos dispositivos pueden ayudar a reducir el LCOE de una planta CSP podría ser útil en un futuro próximo.

NOMENCLATURE

AET	Accelerated Exposure Testing
AM	Air Mass
AU	Astronomical Unit: is a unit of the averaged distance between the Sun and the Earth. Is defined as exactly 149.597.870.700 metres (≈ 150 Million kilometres).
BESS	Battery Energy Storage System
CAPEX	Capital Expenditure
CSIRO	Commonwealth Scientific and Industrial Research Organisation
CSP	Concentrating Solar Power
CSTP	Concentrated Solar Thermal Power
DLR	Deutsches Zentrum für Luft- und Raumfahrt
DNI	Direct Normal Irradiance
FRES	Fluctuating Renewable Energy Sources. Also called Variable Renewable Energy Sources
FSM	Front Surface Mirror
G	Irradiance: Radiant flux incident on the sample surface per unit area. SI-Unit: W/m^2; The spectral solar irradiance or direct solar irradiance is the same concept but takin into account the dependence with the wavelength, is denoted as $G_b(\lambda)$. SI unit: $W/m^2/nm$. 1. The subscript *b* designates beam insolation; the surface orientation is normal to the sun unless otherwise specified by a further subscript. 2. The subscript *d* designates diffuse insolation; the surface orientation is horizontal unless otherwise specified by a further subscript. 3. The subscript *h* designates hemispherical insolation; the surface orientation is horizontal unless otherwise specified by a further subscript. 4. The subscript *o* designates extraterrestrial insolation.
H	Irradiation: incident energy per unit of a surface on a given plane, obtained by integration of irradiance G during a given time interval, usually an hour or a day. SI Unit: MJ/m^2 for a given interval. 3.6 MJ/m^2 = 1 kWh/m^2.
HCE	Heat Collector Element
HTF	Heat Transfer Fluid
I	Radiant Intensity: radiant power per unit solid angle of a light source in any given

	direction. SI-Unit: W/sr
IAM	Incidence Angle Modifier
IC	Intercept Factor
IoT	Internet of Things
IRENA	International Renewable Energy Agency
ISCC	Integrated Solar Combined Cycle
KPI	Key Performance Indicator
L	Radiance: is the emitted radiant intensity by a surface unit of a light source in a direction given by an angle θ. SI Unit: W/steradian/m2
LCOE	Levelized Cost of Electricity
LED	Light Emitting Diode
LFR	Linear Fresnel Reflectors
M	Radiant Emittance or radiant exitance
NIR	Near-Infrared
NIST	National Institute of Standards and Technology
NREL	National Renewable Energy Laboratory
O&M	Operation & Maintenance
OET	Outdoor Exposure Testing
PPT	Percentage Points
PSA	Plataforma Solar de Almería
PTC	Parabolic-Trough Collector
PTG	Photonics Technology Group at the University of Zaragoza
PV	Photovoltaic (plants)
PVD	Physical Vapour Deposition
Ra	Arithmetical Mean Roughness
RMS	Root Mean Square
RU	Reflectance Units
SEGS	Solar Electric Generating Station
sr	Steradian: is the SI-Unit of the solid angle Ω. Is a dimensionless unit. Is the analogue in three dimensions to the radian. The solid angle is related to the area of the spherical surface that it spans. A solid angle of one steradian (sr), is defined as the solid angle that delineates an area on the surface of a reference sphere equal to the radius-squared of that sphere. There are 2π sr in a

	hemisphere.
SSM	Second Surface Mirror
ST	Solar Tower
STE	Solar Thermal Energy
TES	Thermal Energy Storage
TIS	Total Integrated Scattering
TSI	Total Solar Irradiance
USA	United States of America
UV	Ultraviolet
γ_s	Solar azimuth angle
θ	Incidence angle, Acceptance half-angle, half-cone angle
ρ	Reflectivity, an intrinsic property of a material. Reflectance is defined as an extensive property of a material
σ	Standard deviation
φ	Acceptance angle
ϕ	Angular spread, for solar concentrating purpose, angular spread of the concentrated radiation incident on the receiver

TERMS AND DEFINITIONS

Capacity Factor [Cp]	Power output during time t (MWh) / time * rated power (MW)
Concentrator	Reflector surface that focuses sunlight into a receiver
Solar collector	A solar collector is the sum of the receiver, reflector surface, the supporting structure, and its foundation

REFERENCES

[1] M. K. Hubbert, "Nuclear Energy and the Fossil Fuels," *Drilling and Production Practice,* Vols. 1956-January, pp. pp.7-25, 1956.

[2] U. Bardi, "Peak Oil, 20 Years Later: Failed Prediction or Useful Insight?," *Energy Research and Social Science,* vol. 48, no. March 2018, p. 257–261, 2019.

[3] IEA, "World Energy Outlook 2019," Paris, 2019.

[4] British Petroleum, "2018 BP Energy Outlook," British Petroleum, 2018.

[5] K. Lovegrove and W. Stein, Concentrating Solar Power Technology: Principles, Developments and Applications, K. Lovegrove and W. Stein, Eds., Cambridge, UK: Woodhead Publishing Series/Elsevier, 2012, p. 577.

[6] D. Feldman, "Solar Industry Update.," 2020.

[7] IRENA, "Renewable Power Generation Costs in 2019," 2020.

[8] D. Feldman and R. Margolis, "Q4 2019/Q1 2020 Solar Industry Update," NREL, Colorado, 2019.

[9] D. Feldman, "Solar Industry Update. 2020. Golden, CO: National Renewable Energy Laboratory.".

[10] J. Jorgenson, P. Denholm and M. Mehos, "Estimating the Value of Utility-Scale Solar Technologies in California Under a 40% Renewable Portfolio Standard," NREL, Golden, Colorado, 2014.

[11] NREL, "Andasol 1," [Online]. Available: https://solarpaces.nrel.gov/andasol-1.

[12] R. B. Pettit, "Characterization of the Reflected Solar Beam Profile of Solar Mirror Materials," *Solar Energy,* vol. 19, p. 733–741, 1976.

[13] R. B. Pettit and J. M. Freese, "Wavelength Dependent Scattering Caused By Dust Accumulation on Solar Mirrors," *Solar energy materials,* vol. 3, no. 1-2, pp. 1-20, 1980.

[14] A. Fernández García, F. Sutter, M. Montecchi, F. Sallaberry, A. Heimsath, C. Heras, E. Le Baron and A. Soum-Glaude, "Parameters and method to evaluate the reflectance properties of reflector materials for

concentrating solar power technology, SolarPACES Official Reflectance Guideline Version 3.0," SolarPACES, 2018.

[15] AENOR, *UNE 206016:2018, Paneles reflectantes para tecnologías de concentración solar,* Madrid, 2018.

[16] SolarPACES, "Solar Power and Chemical Energy Systems," [Online]. Available: https://www.solarpaces.org/about/solarpaces/.

[17] F. Wolfertstetter, S. Wilbert, F. Terhag, N. Hanrieder, A. Fernandez-García, C. Sansom, P. King, L. Zarzalejo and A. Ghennioui, "Modelling the soiling rate: Dependencies on meteorological parameters," in *AIP Conference Proceedings 2126*, 2019.

[18] K. Ilse, L. Micheli, B. W. Figgis, K. Lange, D. Daßler, H. Hanifi, F. Wolfertstetter, V. Naumann, C. Hagendorf, R. Gottschalg and J. Bagdahn, "Techno-Economic Assessment of Soiling Losses and Mitigation Strategies for Solar Power Generation," *Joule,* vol. 3, no. 10, pp. 2303-2321, 2019.

[19] "Protermosolar. Proyectos Solares en el exterior," [Online]. Available: https://www.protermosolar.com/proyectos-termosolares/proyectos-en-el-exterior/.

[20] UN Data, "Electricity, net installed capacity of electric power plants".

[21] L. Crespo, "The long-term market potential of concentrating solar power (CSP) systems," in *Concentrating solar power technology: Principles, developments and applications*, 2nd ed., Cambridge, UK, Woodhead Publishing Series/Elsevier, 2021, pp. 477-508.

[22] G. Kopp and J. L. Lean, "A new, lower value of total solar irradiance: Evidence and climate significance," *Geophysical Research Letters,* vol. 38, no. 1, pp. 1-7, 2011.

[23] A. Rabl, Active Solar Collectors and Their Applications, New York: Oxford University Press, 1985.

[24] P. Bendt and A. Rabl, "Optical analysis of point focus parabolic radiation concentrators," *Applied optics,* vol. 20, no. 4, pp. 674-683, 1981.

[25] ASTM International, *ASTM G173-03 (2020), Standard Tables for Reference Solar Spectral Irradiances: Direct Normal and Hemispherical on 37° Tilted Surface,* West Conshohocken, PA, 2020.

[26] J. A. Duffie and W. A. Beckman, Solar Engineering of Thermal Processes, Photovoltaics and Wind,

Hoboken, New Jersey: John Wiley & Sons Inc., 2020.

[27] "HOMER Published Solar Data," UL, [Online]. Available: https://www.homerenergy.com/products/pro/docs/latest/published_solar_data.html.

[28] "The POWER Project," NASA, [Online]. Available: https://power.larc.nasa.gov/.

[29] "National Solar Radiation Database," [Online]. Available: http://rredc.nrel.gov/solar/old_data/nsrdb/.

[30] M. Binotti, G. Manzolini and G. Zhu, "An alternative methodology to treat solar radiation data for the optical efficiency estimate of different types of collectors," *Solar Energy,* vol. 110, p. 807–817, 2014.

[31] AENOR, *UNE 206009:2013, Centrales Solares Terminología,* Madrid, 2013.

[32] AENOR, *UNE-EN ISO 9488:2001, Energía solar. Vocabulario,* Madrid, 2001.

[33] A. Heimsath, T. Schmid and P. Nitz, "Angle Resolved Specular Reflectance Measured with VLABS," *Energy Procedia,* vol. 69, pp. 1895-1903, 2015.

[34] A. Heimsath and P. Nitz, "Scattering and specular reflection of solar reflector materials – Measurements and method to determine solar weighted specular reflectance," *Solar Energy Materials and Solar Cells,* vol. 203, no. February, 2019.

[35] H. M. Güven and R. B. Bannerot, "Determination of error tolerances for the optical design of parabolic troughs for developing countries," *Solar Energy,* vol. 36, no. 6, pp. 535-550, 1986.

[36] B. Butler and R. Pettit, "Optical Evaluation Techniques For Reflecting Solar Concentrators," *Proc. SPIE 0114, Optics Applied to Solar Energy Conversion,* no. October 1977, p. 8, 1977.

[37] C. Alcañiz, N. Martínez, C. Heras and I. Salinas, "Study of the Influence of Specularity on the Efficiency of Solar Reflectors," *Energy Procedia,* vol. 69, pp. 14-23, 2015.

[38] B. H.L., C. P.J., G. Jorgensen and R. Pettit, "Solar Reflectance, Transmittance and absorptance of common materials," US DOE, Golden, Colorado, 1979.

[39] A. Z. Hafez, A. Attia, H. S. Eltwab, A. O. ElKousy and e. al, "Design analysis of solar parabolic trough thermal collectors," *Renewable and Sustainable Energy Reviews,* vol. 82, no. June 2017, pp. 1215-1260, 2018.

[40] E. Zarza, "7 - Parabolic-trough concentrating solar power (CSP) systems," in *Concentrating solar power technology: Principles, developments and applications*, Woodhead Publishing, 2012, pp. 197-239.

[41] F. Sutter, S. Meyen, A. Fernández García and P. Heller, "Spectral characterization of specular reflectance of solar mirrors," *Solar Energy Materials and Solar Cells,* vol. 145, pp. 248-254, 2016.

[42] Y. S. Touloukian and D. P. DeWitt, "Volume 7. Thermal Radiative Properties-Metallic Elements and Alloys," in *Thermophysical properties of matter*, vol. 7, Thermophysical Properties Research Center, Purdue University, 1989, pp. 16a, 27a.

[43] R. Birkebak, J. Dawson, B. McCullough and B. Wood, "Hemispherical reflectance of metal surfaces as a function of wavelength and surface roughness," *International Journal of Heat and Mass Transfer,* vol. 10, no. 9, pp. 1225-1232, 1967.

[44] I. Salinas, C. Heras, C. Alcañiz, D. Izquierdo, N. Martínez and R. Alonso, "Portable Solar Spectrum Reflectometer for planar and parabolic mirrors in solar thermal energy plants," *Solar Energy,* vol. 135, pp. 446-454, 2016.

[45] J. Workman, Spectroscopy of solids, Elsevier, 1998, pp. 225-246.

[46] H. Davies, "The reflection of electromagnetic waves from a rough surface," *Proc. IEEE Part IV: Institution Monographs,* vol. 101, no. 7, pp. 209-214, 1954.

[47] A. Pfahl, J. Coventry, M. Röger, F. Wolfertstetter, J. F. Vásquez-Arango, F. Gross, M. Arjomandi, P. Schwarzbözl, M. Geiger and P. Liedke, "Progress in heliostat development," *Solar Energy,* vol. 152, pp. 3-37, 2017.

[48] T. R. Mancini, J. A. Gary, G. J. Kolb and C. K. Ho, "Power Tower Technology Roadmap and cost reduction plan," Sandia Labs, DOE, USA, 2011.

[49] P. Heller, The performance of concentrated solar power (CSP) systems: analysis, measurement and assessment, Elsevier Inc., 2017, pp. 1-290.

[50] J. Vitko Jr. and J. Shelby, "Solarization of Heliostat Glasses," Sandia Laboratories, Albuquerque, New Mexico, 1980.

[51] F. Buendía-Martínez, A. Fernández-García, F. Sutter, J. Wette, L. M. Arcos and T. J. Reche-Navarro, "Effect of the solarization in concentrating solar thermal components," CIEMAT-DLR, 2020.

[52] F. Sutter, A. Fernández García, P. Heller, K. Anderson, G. Wilson, M. Schmücker and P. Marvig, "Durability Testing of Silvered-Glass Mirrors," *Energy Procedia,* vol. 69, pp. 1568-1577, 2015.

[53] C. Kennedy, "Advances in concentrating solar power collectors: mirrors and solar-selective coatings," *Vac. Tech. & Coating,* vol. 6103, no. October, 2008.

[54] G. Jorgensen, C. Kennedy, D. King and K. Terwilliger, "Optical Durability Testing of Candidate Solar Mirrors," *NREL/TP-520-28110,* no. March, pp. 1-58, 2000.

[55] A. García-Segura, A. Fernández García, M. J. Ariza, F. Sutter and L. Valenzuela, "Durability studies of solar reflectors: A review," *Renewable and Sustainable Energy Reviews,* vol. 62, pp. 453-467, 2016.

[56] A. G. Website, "Alanod, solar reflective surfaces," ALANOD GmbH & Co. KG, [Online]. Available: https://alanod.com/en/products.

[57] T. Fend, G. Jorgensen and H. Küster, "Applicability of highly reflective aluminium coil for solar concentrators," *Solar Energy,* vol. 68, no. 4, pp. 361-370, 2000.

[58] C. Kennedy, "Solar Annual Review Meeting; CSP Advanced Systems: Optical Materials," NREL, DOE, Austin, Texas, 2008.

[59] A. Heimsath, G. Kutscheidt and P. Nitz, "Measuring reflectance - overview and influence on optical performance," *SolarPACES,* vol. 2011, 2011.

[60] M. Brogren, B. Karlsson, A. Roos and A. Werner, "Analysis of the effects of outdoor and accelerated ageing on the optical properties of reflector materials for solar energy applications," *Solar Energy Materials and Solar Cells,* vol. 82, no. 4, pp. 491-515, 2004.

[61] F. Sutter, A. Fernández García, P. Heller, R. López-Martín, S. Meyen and R. Pitz-paal, "Methods for Service Life Time Estimation of Aluminum Reflectors," in *SolarPACES 2011*, 2011.

[62] F. Sutter, S. Ziegler, M. Schmücker, P. Heller and R. Pitz-Paal, "Modelling of optical durability of enhanced aluminum solar reflectors," *Solar Energy Materials and Solar Cells,* vol. 107, pp. 37-45, 2012.

[63] C. Sansom, A. Fernández García, F. Sutter, H. Almond, P. King and L. Martínez-Arcos, "Soiling and cleaning of polymer film solar reflectors," *Energies,* vol. 9, no. 12, 2016.

[64] C. E. Kennedy and K. Terwilliger, "Optical Durability of Candidate Solar Reflectors," *J. Sol. Energy Eng.,*

vol. 127(2), pp. 262-269, 2005.

[65] US DOE, "Collectors R&D for CSP Systems," Office of Energy Efficiency and Renewable Energy, 2020. [Online]. Available: https://www.energy.gov/eere/solar/collectors-rd-csp-systems.

[66] G. Nilsen, "Development of an Abrasion-Resistant Antisoiling Coating for Front-Surface Reflectors," *Sundog Solar Technology,* 2017.

[67] A. Fernández-García, F. Sutter, L. Martínez-Arcos, L. Valenzuela and C. Sansom, "Advanced mirror concepts for concentrating solar thermal systems," *Advances in Concentrating Solar Thermal Research and Technology,* pp. 29-43, 2017.

[68] A. M. Patnode, Simulation and performance evaluation of parabolic trough solar power systems (Mechanical Engineering), University of Wisconsin-Madison, 2006.

[69] A. Colmenar-Santos, F. J. Munuera-Pérez, M. Tawfik and M. Castro-Gil, "A simple method for studying the effect of scattering of the performance parameters of Parabolic Trough Collectors on the control of a solar field," *Solar Energy,* vol. 99, pp. 215-230, 2014.

[70] F. Sutter, M. Montecchi, H. von Dahlen, A. Fernández García and M. Röger, "The effect of incidence angle on the reflectance of solar mirrors," *Solar Energy Materials and Solar Cells,* vol. 176, no. November 2017, pp. 119-133, 2018.

[71] G. Zhu, "Study of the optical impact of receiver position error on parabolic trough collectors," *Journal of Solar Energy Engineering,* vol. 135, no. 3, pp. 1-5, 2013.

[72] M. Binotti, G. Zhu, A. Gray, G. Manzolini and P. Silva, "Geometric analysis of three-dimensional effects of parabolic trough collectors," *Solar Energy,* vol. 88, pp. 88-96, 2013.

[73] D. J. Griffith, L. Vhengani and M. Maliage, "Measurements of Mirror Soiling at a Candidate CSP Site," *Energy Procedia,* vol. 49, pp. 1371-1378, 2013.

[74] F. Wolfertstetter, K. Pottler, A. A. Merrouni, A. Mezrhab and R. Pitz-paal, "A Novel Method for Automatic Real-Time Monitoring of Mirror Soiling Rates," in *SolarPACES Concentrated Solar Power and Chemical Energy Systems*, 2012.

[75] P. Bellmann, F. Wolfertstetter, R. Conceição and H. G. Silva, "Comparative modeling of optical soiling losses for CSP and PV energy systems," *Solar Energy,* vol. 197, no. January, pp. 229-237, 2020.

[76] A. Fernández García, F. Sutter, L. Martínez-Arcos, C. Sansom, F. Wolfertstetter and C. Delord, "Equipment and methods for measuring reflectance of concentrating solar reflector materials," *Solar Energy Materials and Solar Cells,* vol. 167, no. August, pp. 28-52, 2017.

[77] C. A. Arancibia-Bulnes, M. I. Peña-Cruz, A. Mutuberría, R. Díaz-Uribe and M. Sánchez-González, "A survey of methods for the evaluation of reflective solar concentrator optics," *Renewable and Sustainable Energy Reviews,* vol. 69, no. October 2015, pp. 673-684, 2017.

[78] R. B. Pettit, "Characterizing solar mirror materials using portable reflectometers," Sandia National Laboratories, Albuquerque, NM, 1982.

[79] M. Montecchi, "Approximated method for modelling hemispherical reflectance and evaluating near-specular reflectance of CSP mirrors," *Solar Energy,* vol. 92, pp. 280-287, 2013.

[80] J. Räty, K.-E. Peiponen and T. Asakura, "UV-Visible Reflection Spectroscopy of Liquids," in *Springer Series in optical sciences*, Heidelberg, Springer, 2004, p. 220.

[81] J. Workman and A. W. Springsteen, "Appendix A: Sources, detectors, and window materials for UV-VIS, NIR, and IR Spectroscopy," in *Applied Spectroscopy: a compact reference for practitioners*, London, Academic Press Limited, 1998.

[82] N. Martinez, R. Navio, C. Heras, I. Salinas and M. Mainar, "A New Portable Specular Reflectometer, Condor: Description, laboratory and field tests," in *SolarPACES*, 2012.

[83] A. Heimsath, T. Schmidt, J. Steinmetz, C. Reetz, M. Schwandt, R. Meyer and P. Nitz, "Automated monitoring of soiling with AVUS instrument for improved solar site assessment," *AIP Conference Proceedings,* vol. 2033, no. November 2018, p. 7, 2018.

[84] R. Calvo, D. Arguelles Arizcun and A. Fernández García, "Innovative low-cost sensor for continuous soiling monitoring of CSP plants," *SolarPaces Conference,* 2013.

[85] C. Villasante, C. Zuazo, M. Sanchez, J. G. Barbarena, G. Pérez and J. Ubach, "SMARTMIRROR ® : Making CSP plants smarter and more profitable," *SolarPACES Conference,* 2020.

[86] E. U. H. 2020, "SOLWARIS: Solving Water Issues for CSP Plants," [Online]. Available: https://solwaris.eu/.

[87] J. Fernández-Reche, "Reflectance measurement in solar tower heliostats fields," *Solar Energy,* vol. 80, no. 7, pp. 779-786, 2006.

[88] A. Fernández García, «Estudio de la reflectancia especular en plantas de captadores solares cilindroparabólicos,» CIEMAT, Madrid, 2012.

[89] M. Hollander and D. Woffe, "Nonparametric Statistical Methods," in *Second ed. Wiley-Interscience*, New York, 1999.

[90] Schott GmbH, "SCHOTT AMIRAN® - anti-reflective glass for façades," Schott GmbH, [Online]. Available: https://www.schott.com/architecture/spanish/products/anti-reflective-glass/amiran.html.